Published in final edited form as:

J Immunol. 2019 May 15; 202(10): 2873–2887. doi:10.4049/jimmunol.1801577.

Trogocytosis-mediated Intracellular Signaling in CD4+ T cells Drives T_H2-associated Effector Cytokine Production and Differentiation[1,,2]

Jim Reed[†] and **Scott Wetzel**[*,†,§]

[†]Program in Cellular, Molecular and Microbial Biology, Division of Biological Sciences, University of Montana, Missoula, MT 59812, USA

[§]Center for Environmental Health Sciences, University of Montana, Missoula, MT 59812, USA

Abstract

CD4$^+$ T cells have been observed to acquire APC-derived membrane and membrane-associated molecules through trogocytosis in diverse immune settings. Despite this, the consequences of trogocytosis on the recipient T cell remain largely unknown. We previously reported that trogocytosed molecules on CD4$^+$ T cells engage their respective surface receptors, leading to sustained TCR signaling and survival after APC removal. Using peptide-pulsed BMDC and transfected murine fibroblasts expressing antigenic MHC:peptide complexes as APC, we show that trogocytosis-positive CD4$^+$ T cells display effector cytokines and transcription factor expression consistent with a T_H2 phenotype. *In vitro* polarized T_H2 cells were found to be more efficient at performing trogocytosis than T_H1 or non-polarized CD4$^+$ cells, while subsequent trogocytosis-mediated signaling induced T_H2 differentiation in polarized T_H1 and non-polarized cells. Trogocytosis-positive CD4$^+$ T cells generated *in vivo* also display a T_H2 phenotype, in both TCR-transgenic and wild type models. These novel findings suggest that trogocytosis-mediated signaling impacts CD4$^+$ T cell differentiation and effector cytokine production, and may play a role in augmenting or shaping a T_H2-dominant immune response.

Keywords

Trogocytosis; CD4$^+$ T cell; T_H2; IL-4; effector cytokine; intracellular signaling; cell differentiation; mouse

1. Work funded by R03AI122167 and University of Montana Small Grant program (to S.A.W). Fluorescence Cytometry and Molecular Histology and Florescence imaging core facilities used to perform studies are supported by P30RR033379.

2. Abbreviations used:

[*]**Corresponding Author:** Dr. Scott A. Wetzel, Ph. (406) 243-2168, FAX: (406) 243-4304, scott.wetzel@umontana.edu.

BMDC, bone marrow-derived dendritic cells; FKBP, FK506-binding protein; ICS, Intracellular cytokine staining; Lck, P56Lck; MFI, mean fluorescence intensity; MCC, moth cytochrome-c; OVA, ovalbumin; pZAP-70, phosphotylated ZAP-70; Trog (+), trogocytosis-(positive); Trog (–), trogocytosis-(negative)

Introduction

T lymphocytes acquire lipids and membrane-bound molecules directly from the surface of antigen presenting cells (APC) in a phenomenon termed trogocytosis (1, 2). This event has been frequently observed in $CD4^+$ T-helper (T_H) (3–10), $CD8^+$ (1, 7, 11–13), and γδ (14) T cells. Though the consequences of trogocytosis on recipient cells are not completely understood, it has been described as “an inherent feature in $CD4^+$ T cell activation” (15). This phenomenon is not exclusive to T cells, as B cells (16, 17), NK cells (18–20), basophils (21), macrophages (22, 23), neutrophils (24–26), and dendritic cells (27, 28), have all been reported to perform trogocytosis. With elevated levels of trogocytosis documented in sites of autoimmune inflammation (29), viral and parasitic infections (30–32), rheumatoid arthritis (33), and in tumor environments (34, 35), this widely observed event has been proposed to play a role in the modulation of immune responses (27, 36–41).

Work over the past decade has begun to decipher the mechanism of T cell trogocytosis. We, and others, have previously shown that trogocytosis by $CD4^+$ T cells occurs at the immunological synapse formed between Ag-specific $CD4^+$ T cells and APC (4, 42–45). The formation of the immunological synapse involves the spatio-temporal rearrangement of the TCR, costimulatory molecules, and adhesion molecules, into distinct, spatially-segregated supramolecular activation complexes (SMACs) (46–49). Upon binding MHC:peptide complexes, TCRs migrate towards the center of the SMAC where they become internalized by the T cell and are either recycled to the surface, or ubiquitinated leading to their degradation (50). Martinez-Martin *et al.* have proposed a model of trogocytosis in which APC-derived membrane and membrane proteins are internalized in tandem with TCR via T-cell phagocytosis. Recycling endosomes containing acquired APC fragments then fuse with the T cell plasma membrane resulting in APC-derived molecules being displayed on the T cell surface in their native topological orientation (51, 52). Trogocytosed molecules are retained in a focused spot on the $CD4^+$ T cell surface (4, 10) and remain fully functional, as demonstrated by the ability for trogocytosis-positive ($trog^+$) T cells to present antigen, in the context of other acquired molecules, to responding T cells (6, 8, 9, 15, 36, 53–58). The consequences of such presentation appear to correlate with the nature of the acquired molecules and phenotype of the $trog^+$ cell. While $trog^+$ $CD4^+$ cells displaying acquired CD80 and MHC:peptide have been shown to activate responding naïve T cells (8, 15, 56, 59), presentation of Ag to activated cells has been reported to induce responder cell death (60). In a regulatory context, $trog^+$ T regulatory (T_{reg}), or T_H cells displaying trogocytosed molecules associated with immune-suppression, such as HLA-G, show enhanced suppressive capabilities (15, 38, 54, 61–63). Collectively, the above findings underscore that $CD4^+$ T cell trogocytosis, and the subsequent presentation of acquired molecules, are biologically significant events in the context of regulating immune responses. While the ability of $trog^+$ T cells to act as APC has been fairly well documented, much less is known about the biological consequences of trogocytosis on an individual $trog^+$ cell. In our previous studies, we detected TCR signaling in $trog^+$, but not $trog^–$, $CD4^+$ T cells up to 72 hours after separation from APC. This sustained signaling was mediated by trogocytosed molecules engaging their cognate receptors on the $trog^+$ T cell, resulting in “autopresentation”, referred to here as “trogocytosis-mediated signaling”. This signaling led

to the enhanced survival of trog$^+$ cells compared to trog$^-$ cells, up to five days after APC removal (10). Consistent with these findings, Zhou *et al.* found that trog$^+$ CD4$^+$ T cells displayed sustained activation of NFκB and AP1, 24 hours after removal from APC. Interestingly, the trog$^+$ cells also developed a unique cytokine profile (64), raising the possibility that a difference exists between trogocytosis-mediated signaling and signals received from APC. Taken together, the above results suggest that trogocytosis-mediated signaling has the potential to uniquely impact the survival, activation state, and effector cytokine production and/or maintenance of the trog$^+$ CD4$^+$ T cell after separation from APC.

In this study, we examined whether trogocytosis-mediated signaling impacted T cell effector cytokine production and differentiation in the context of the individual trog$^+$ cell. Using non-polarized *in vitro* CD4$^+$ T cell blasts, we found that shortly after APC removal, a high frequency of trog$^-$ cells expressed IFNγ, consistent with a T helper 1 (T_H1) phenotype. The trog$^-$ cells did not maintain IFNγ expression over a subsequent 72-hour incubation, and by 72 hours only minimal levels of any effector cytokine examined were detected. In contrast, 5 hours after APC removal the frequency of IFNγ$^+$ trog$^+$ cells was significantly lower than IFNγ$^+$ trog$^-$ cells. Interestingly, over the subsequent 72-hour incubation, IL-4 expression was significantly increased in the trog$^+$ cells, consistent with a T_H2 phenotype. Because trogocytosis-mediated signaling induces preferential survival of trog$^+$ cells (10), the appearance of the T_H2 phenotype by trog$^+$ cells could be due to differences in the ability of T_H1 and T_H2 cells to perform trogocytosis. Consistent with this possibility, *in vitro* polarized T_H2 cells were more efficient at performing trogocytosis than T_H1 or non-polarized CD4$^+$ cells. However, further investigation revealed that trogocytosis-mediated signaling was directly contributing to the T_H2-associated effector cytokine and transcription factor expression in non-polarized trog$^+$ CD4$^+$ cells. In addition, *in vitro* T_H1-polarized trog$^+$ cells lost expression of IFNγ and T-bet, and began expressing IL-4 and GATA-3, suggesting that trogocytosis-mediated signaling was inducing T_H1 to T_H2 conversion. Finally, using both TCR-transgenic and non-transgenic models, and distinct Ag systems, we show that *in vivo*, a significantly higher frequency of trog$^+$ CD4$^+$ T cells display a T_H2 phenotype when compared to trog$^-$ cells from the same animal. Cumulatively, these findings suggest that trogocytosis-mediated signaling has the potential to significantly impact CD4$^+$ T cell effector cytokine production and differentiation, and subsequently may play a role in sustaining, augmenting, or shaping, T_H2-dominant immune responses.

Materials and Methods

Animals

B10.A and C57BL/6 CD45.1 mice were purchased from The Jackson Laboratory (Sacramento, CA). 5C.C7 TCR (Vβ3$^+$) transgenic Rag-1$^{-/-}$ mice specific for pigeon cytochrome c fragment 88–104 and reactive against moth cytochrome c (MCC) fragment 88–103 (65) were purchased from Taconic (Rensselaer, NY). For some experiments, 5C.C7 mice were crossed with B10.A mice and the splenocytes from F1 generation animals were used. Both male and female mice were used in this study, and no differences were observed between male and female T cell phenotypes. Mice were housed in the University of

Montana Laboratory Animal Resources facility and were allowed food and water *ad libitum*. All procedures were supervised and in accordance with the University of Montana Institutional Animal Care and Use Committee.

Antibodies and reagents

The following conjugated or unconjugated antibodies were purchased from: Biolegend (San Diego, CA): anti-CD3 (145–2C11), anti-CD4 (RM4–5), anti-CD69 (H1.2F3), anti-CD80 (16–10A1), anti-Foxp3 (150D), anti-I-E^k (17–3-3), anti-IA/IE (M5/114.15.2), anti-IFNγ (XMG1.2), anti-IL-2 (JES6–5H4), anti-IL-4 (11B11), anti-IL-6 (MP5–20F3), anti-IL-9 (RM9A4), anti-IL-17A (TC11–18H10.1), anti-IL-21 (FFA21), anti-Bcl-6 (IG19E/A8), anti-T-bet (4B10), anti-GATA-3 (16E10A23), Streptavidin (PE-Dazzle594). Conjugated or unconjugated antibodies were also purchased from BD Biosciences (Franklin Lakes, NJ): anti-pZAP-70 (17A/P-ZAP-70), anti-Vβ3 (KJ25), anti-IL-12 (C15.6), anti-CD80 (16–10A1), anti-CD86 (GL1), anti-CD90.2 (30-H12)], and eBiosciences (San Diego, CA): anti-IL-5 (TRFK5), anti-IL-10 (JES5–16E3), anti-RORγt (AFKJS-9). AlexaFluor 488- and AlexaFluor 647-conjugated Streptavidin were purchased from Jackson ImmunoResearch Laboratories (West Grove, PA).

Whole pigeon cytochrome c (PCC) and Ovalbumin (Ova) proteins were obtained from Sigma-Aldrich (St. Louis, MO) and moth cytochrome C fragment 88–103 ($MCC_{88–103}$) peptide was obtained from Genscript (Piscataway, NJ). Peptides were dissolved in sterile nano-pure water at 500 μM and aliquots were stored at −80 °C until used.

Culture Media

Fibroblast APC were cultured in DMEM (Life Technologies, Carlsbad, CA) supplemented with 10% FBS (Atlanta Biologicals, Atlanta, GA), 1 mM L-glutamine, 100 mg/ml sodium pyruvate, 50 mM 2-ME, essential and nonessential amino acids (Life Technologies), 100 U/ml penicillin G, 100 U/ml streptomycin, and 50 mg/ml gentamicin (Sigma-Aldrich).

Primary splenocytes, T lymphocytes, and bone marrow-derived dendritic cells (BMDC) were maintained in complete RPMI which consisted of RPMI 1640 medium (Life Technologies) supplemented with 10% FBS (Atlanta Biologicals, Flowery Branch, GA), 1 mM L-glutamine, 100 mg/ml sodium pyruvate, 50 mM 2-ME, essential and nonessential amino acids (Life Technologies), 100 U/ml penicillin G, 100 U/ml streptomycin, and 50 mg/ml gentamicin (Sigma-Aldrich).

Antigen Presenting Cells

In *in vitro* trogocytosis experiments, peptide-pulsed B10.A BMDC or the previously described MCC:FKBP cell line (4) were used as APC. The MCC:FKBP is a $CD80^{high}$ Ltk^- fibroblast cell line that has been transfected with ICAM-1, I-E^k α-chain, and an I-E^k β-chain with covalently attached antigenic $MCC_{88–103}$ peptide via a flexible linker, and a cytoplasmic tail containing 3 copies of FK506-binding protein (Ariad Pharmaceuticals, Cambridge, MA). This cell line expresses levels of CD80 and ICAM-1 comparable to B10.BR splenocyte APC (4).

Generation of BMDCs

Bone marrow cells were isolated from femurs and tibiae of B10.A mice and cultured for 6 days in sterile non-tissue culture grade petri dishes at 10^5 cells/ml in complete RPMI medium containing 30 ng/ml recombinant murine granulocyte macrophage-colony stimulating factor (GM-CSF) (PeproTech, Rocky Hill, NJ) at 37 °C and 5% CO_2. Fresh culture media and GM-CSF were added on day 3, and non-adherent cells were harvested on day 6. Cells were activated by plating on tissue culture-coated 6-well plates with addition of Sigma adjuvant system at 125 ng/ml 18 hours prior to use. Adherent cells were surface biotinylated and exogenously loaded with $MCC_{88–103}$ peptide at a final concentration of 2.5 μM for 2 hours prior to use. Purity was verified via flow cytometry to be >90% $CD11c^+$.

In vitro T cell priming

Non-polarized TCR-transgenic $CD4^+$ T cell blasts were generated *in vitro* to increase the potential for trogocytosis relative to naïve $CD4^+$ T cells (42). Single-cell suspensions of splenocytes from 6- to 12-week-old 5C.C7 or 5C.C7 x B10.A F1 transgenic mice were depleted of erythrocytes by hypotonic lysis using Gey's balanced salt solution (155 mM NH_4Cl, 10mM $KHCO_3$) and resuspended in complete RPMI 1640. Splenocytes from 5C.C7 x B10.A F1 mice were activated *in vitro* for 6 days by addition of 2.5 μM $MCC_{88–103}$ peptide to splenic cell suspensions. 5C.C7 splenocytes were stimulated for 48 hours on pre-coated anti-CD3 (1 μg/ml) and anti-CD28 (1 μg/ml) plates followed by a 2 day incubation after removal from antibody-coated plates prior to use. Viable lymphocytes were isolated from priming cultures by density centrifugation using Lympholyte M (Cedarlane Labs, Burlington, NC). When culturing B10.A x 5C.C7 F1 or C57BL/6 cells, B cells were depleted from cultures by incubating cells for 30 min with biotin-labeled anti-B220 (BioLegend), followed by 3 washes in PBS. Cells were then incubated for 20 min with 3.75 μm streptavidin-coated magnetic particles (Spherotech) followed by removal of $B220^+$ cells by magnetic separation. Cultures of cells from peptide T cell blast cultures were 90–95% $CD4^+$ immediately prior to use in the trogocytosis-assay.

In vitro T_H1 and T_H2 polarization

To induce T_H1 or T_H2 effector subset polarization, primary T cells were stimulated directly *ex vivo* on anti-CD3 (1 μg/ml) and anti-CD28 (1 μg/ml) coated plates, as described above, with either T_H1 (5 ng/ml IL-12 and 20 μg/ml anti-IL-4 (11B11), or T_H2 (10 ng/ml rmIL-4 and 20 μg/ml anti-IFNγ) differentiation cocktails (66). On day 2, 5 U/ml rmIL-2 was added to all cultures. The exogenous cytokines were obtained from Peprotech, (Rocky Hill, NJ) and neutralizing antibodies were purchased from Biolegend. Cells were removed from Ab-coated plates on day 4. Polarization was confirmed through flow cytometry analysis of transcription factor and cytokine staining for GATA-3, T-Bet, IL-4 and IFNγ. Immediately prior to use in the trogocytosis assay, >95% of $CD4^+$ blasts generated under T_H1-polarizing conditions were T-bet^+, and >60% of $CD4^+$ blasts generated under T_H2-polarizing conditions were GATA-3^+.

Standard *in vitro* trogocytosis assay

To assess trogocytosis by the $CD4^+$ 5C.C7 T cells, we used our previously described standard *in vitro* trogocytosis assay ((10) Fig. S1A). Briefly, 0.5×10^6 MCC:FKBP fibroblast or 1×10^6 BMDC APC cells were surface biotinylated using EZ-Link Sulfo-NHS-Biotin (Thermo Scientific, Waltham, MA) and then plated into individual wells of a 6-well tissue culture plate (Greiner, Monroe, NC) and incubated overnight at 37 °C. The MCC:FKBP cell line doubling time is approximately 12 hours, so following the overnight incubation wells contained 10^6 APC at the time T cells were added. To facilitate magnetic depletion of APC from recovered T cells, iron-containing polystyrene 2.22 μm beads (Spherotech, Green Oaks, IL) were added to the overnight cultures at a final concentration of 0.01% w/v. Twelve to 18 hours later, free magnetic beads were removed from cultures by rinsing, and 2.5×10^6 *in vitro*-primed T cells (for a final 2.5:1 T:APC ratio), were added to each well and subsequently incubated for 90 min at 37 °C. After the 90-min incubation T cells were recovered from the cultures by rinsing with PBS. Greater than 95% of residual APC were removed by magnetic separation and greater than 70% of the input T cells were routinely recovered from the culture at 90 min after the PBS wash. After two additional PBS washes, recovered T cells (containing both $trog^+$ and $trog^-$ cells) were analyzed immediately by flow cytometry, or were resuspended in complete RPMI 1640 medium at low density (10^4 /ml) to minimize T:T contact, and cultured for additional time periods. These cultures of recovered cells contained >95% $CD4^+$ cells, and <0.1% residual APC (Fig. S1B).

Inhibition of TCR signaling

To confirm the role of trogocytosis-mediated signaling in effector function, TCR signaling was extinguished using the reversible Src family tyrosine kinase inhibitor PP2 (Life Technologies), as previously reported (10, 67). Immediately post-trogocytosis assay, recovered T cells were incubated for 20 min in 20 μM PP2, followed by three washes in PBS to remove the PP2. Cells were then assessed immediately to confirm the treatment halted all TCR-signaling, or were cultured as described above and assessed for TCR-downmodulation, transcription factor, and intracellular cytokine expression via flow cytometry.

CFSE labeling

Primary mouse splenocytes were washed 2x with CFSE loading buffer (0.1% FBS in PBS pH 7.4). Cells were then resuspended at 10^7 cells/ml in pre-warmed CFSE loading buffer containing 5 μM CFSE (Sigma-Aldrich) and incubated at 37 °C for 10 minutes. The reaction was stopped by addition of an equal volume of complete RPMI 1640 medium containing 10% FBS, followed by two additional washes in complete RPMI.

In vivo trogocytosis experiments

In adoptive transfer experiments, B10.A mice were immunized via base of tail subcutaneous injection with either 300 μg pigeon cytochrome c (PCC) protein (Sigma-Aldrich) in 100 μl of Sigma Adjuvant System (SAS) or with 100 μl of PBS as a negative control. 24 hours later, 2×10^6 CFSE labeled 5C.C7 primary splenocytes in PBS were injected i.v. . Draining inguinal lymph nodes were collected five days post-adoptive transfer and analyzed using

flow cytometry. Donor 5C.C7 cells were identified as being Vβ3$^+$ and CFSE$^+$. Of these transferred donor cells, trog$^+$ cells were identified as CD3$^+$ CD4$^+$ CD80$^+$ I-E^{k+} (Fig. S1 D).

To generate *in vivo* trog$^+$ cells in a non-transgenic setting, C57Bl/6 CD45.1 mice were subcutaneously immunized at the base of tail with 300 μg of chicken egg white albumin (OVA) (Sigma-Aldrich) in 100 μl SAS, or 100 μl SAS alone as a control. 14 days later, OVA-immunized mice were boosted s.c. with 300 μg OVA in 100 μl of PBS, control mice were injected with 100 μl PBS alone. Five days post-boost, draining inguinal lymph nodes and spleens were harvested and analyzed via flow cytometry. Trog$^+$ cells were identified as CD3$^+$ CD4$^+$ CD80/86$^+$ I-A/E$^+$ (Fig. S1 D). To confine analysis of cytokine and transcription factor expression to cells with similar activation states, CD4$^+$ CD69^{High} cells were gated on prior to identification of trog$^+$ and trog$^-$ populations.

Flow cytometry

Cells were recovered from cultures and resuspended at 10^6 /ml in FACS buffer (PBS pH 7.4 containing 2% BSA Fraction V (Sigma-Aldrich), 2.5 mM EDTA, and 0.1% NaN_3). To assess viability of cells, cells were stained for 10 min at RT with Zombie NIR fixable viability dye (Biolegend) diluted in PBS then washed 3x with PBS. Cells were then stained for surface markers with the indicated reagents for 30 min on ice in FACS buffer. After three additional washes in FACS buffer, cells were stained for 20 min with secondary reagents in FACS buffer, when necessary. Following a final set of three washes in FACS buffer, cells were resuspended in 400 μl of FACS buffer and stored on ice until being analyzed within 2 hours of staining. Alternatively, cells were fixed in ice-cold fixative (4% paraformaldehyde and 0.5% glutaraldehyde), or Biolegend Fixation Buffer, for 30 min at 4 °C followed by 3 washes in FACS buffer. Fixed cells were resuspended in 400 μl of FACS buffer and stored in the dark at 4 °C until being analyzed the following day.

To enhance detection of intracellular cytokines, in Figs. 2, 4A-C, 6, 7, and 8, cells were re-stimulated at for 5 hours 37 °C with 500 ng/ml PMA (Phorbol 12-myristate 13-acetate) (Sigma-Aldrich), 1 μg/ml Ionomycin (Sigma-Aldrich), in the presence of 5 μg/ml brefeldin A (BioLegend). After staining surface molecules on live cells, as described above, cells were fixed for 30 min in BD Bioscience cytofix/cytoperm followed by three washes in 1x Biolegend permeabilization/wash buffer (PWB). Cells were then stained for intracellular targets for 60 min on ice or overnight at 4 °C with staining reagents diluted in 1x PWB. Following intracellular staining, cells were washed three times in PWB and were either analyzed immediately, or were stored in FACS buffer in the dark at 4 °C and analyzed the following day.

For transcription factor staining, live cells were stained for surface molecules, as described above, then fixed in Biolegend True-Nuclear transcription factor fixation buffer for 60 min at room temperature. Following 3 washes in True-Nuclear Perm Buffer, intercellular targets cells were stained with antibodies diluted in True-Nuclear Perm Buffer for 60 minutes on ice, or overnight at 4 °C. After a final set of 3 washes in Perm Buffer, cells were resuspended in 300 μl FACS buffer and analyzed immediately via flow cytometry.

Cells were analyzed on a FACSAria (BD Bio-sciences) in the University of Montana Fluorescence Cytometry Core, or an LSRII (BD Bio-sciences) in the University of Montana Center for Translational Medicine. Data were analyzed with FlowJo 8.8.7 and FlowJo 10 software (Tree Star, Ashland, OR). Geometric mean flourescence intensity (MFI) values were determined, where indicated.

Identification of trog$^+$ cells was done by gating on lymphocyte population (SSC-A vs. FSC-A) followed by rigorous doublet exclusion (FSC-W vs. FSC-H, and SSC-W vs. SSC-A). Live CD3$^+$ CD4$^+$ cells were identified by the absence of fixable live/dead staining, and trog$^+$ cells were identified by the presence of trogocytosed biotinylated-APC membrane protein (greater than stained, unstimulated controls) (Figs. 1–7), trogocytosed CD80/CD86 + I-E^k for experiments using 5C.C7 TCR transgenic mice, or presence of CD80/CD86 + MHCII I-A/E for experiments using C57BL6/J mice (Fig. S1). Ag-specific staining was confirmed by comparison to respective isotype controls of matched populations.

Intracellular cytokines and transcription factor gating was established using matched-isotype control Ab staining for respective populations. Trog$^+$ and trog$^-$ isotype control intensities were nearly identical, and vertical lines in histogram data depict fluorescence intensity greater than 99% of cells stained with isotype controls.

Detection of extracellular cytokines

The detection of secreted cytokines in culture medium was performed using BioLegend LEGENDplex beads according to the manufacturer's directions. Briefly, culture medium from cells was centrifuged to remove contaminating cells and debris, and immediately stored at −80 °C until used. Samples and known standards for each cytokine analyzed were subsequently incubated with cytokine-capture beads and biotinylated-detection antibodies in polypropylene microfuge tubes shaking at 1000 rpm at room temperature for 2 hours. Following this incubation, SA-PE was added, followed by a 30 min incubation while shaking at 1000 rpm. Beads were washed and immediately analyzed via flow cytometry.

LEGENDplex beads were analyzed on an LSRII (BD Bio-sciences). Standard curves were generated and data were analyzed with LEGENDplex software (Biolegend/ VigeneTech). Cytokine levels in samples were confirmed using BioLegend LEGEND MAX sandwich cytokine-capture ELISA kits according to manufacturer's protocol.

Microscopic analysis

T cells recovered and isolated from the standard *in vitro* trogocytosis assay were cultured at low density (10^4 cells/ml) for three days in complete RPMI at 37 °C. Live cells were isolated using Lympholyte M density centrifugation prior to detection of trogocytosed molecules with fluorochrome-conjugated streptavidin and anti-I-E^k antibodies diluted in FACS buffer for 30 min on ice. Cells were then washed 3x in PBS and ~10^6 recovered T cells were placed in 0.01% poly-L-lysine (Sigma) precoated #1.5 LabTek II eight-chambered coverslips (Nunc) for 10 min at 37 °C in PBS. Cells were fixed with ice-cold fixative (4% paraformaldehyde and 0.5% glutaraldehyde in PBS) in a dark, a humidified chamber for 20 min at room temperature, followed by permeabilization with 0.2% Triton X-100 in PBS for 10 min. Intracellular cytokine and phospho-ZAP70 staining was

performed for 1 hour at room temperature in a dark humidified chamber followed by washing with PBS and addition of SlowFade Gold anti-fade reagent (Thermo Fisher, Eugene, OR). 0.3 μm optical sections were collected, on an Olympus Fluoview FV1000 laser scanning confocal mounted on an inverted IX81 microscope using a Nikon 60x objective with 1.4 N.A, housed in the UM Molecular Histology and Fluorescent Imaging core facility.

Image analysis

Constrained, iterative deconvolution was performed using the Applied Precision SoftWorx software package (GE Healthcare, Issaquah, WA). The integrated intensity of streptavidin, which is a measure of the amount of fluorescently labeled molecules trogocytosed, was obtained for areas ≥ than six times above background fluorescence. For analysis of phosphorylated ZAP-70, the integrated intensity and mean fluorescent intensity was obtained for areas 6-fold above background. Between 25 and 55 trog$^+$ cells were imaged in each of five independent experiments.

Cells were selected for analysis by the presence of streptavidin or I-E^k (6-fold above background intensity). Unstimulated cells were also stained and examined to establish levels of background and non-specific staining. To determine IL-4 polarization towards trogocytosed molecules, cells were divided into 4 quadrants using the ImageJ quadrant picker plugin, with trogocytosed molecules in the center of one radian along the circumference of the cell. The presence of IL-4 staining in the same quadrant as trogocytosed molecules was defined as specific accumulation. Images presented are maximum intensity projections of three consecutive 0.3 μm-thick Z-axis optical sections centered around the highest intensity staining of trogocytosed molecules on the cells surface were created by stacking images in ImageJ. Additional images presented in Fig. S4 are single 0.3 μm-thick optical sections.

Statistical analysis and graphing

Statistical analysis was determined by student's t test, and one-way ANOVA followed by Tukey's multiple comparison test (Figs. 3E, 7F), using Prism 4 (GraphPad Software, La Jolla, CA). Significance was defined as * $p \leq 0.05$, ** $p \leq 0.01$, *** $p \leq 0.001$, and **** $p \leq 0.0001$.

Results

Intracellular TCR signaling and elevated activation is maintained in trog$^+$, but not trog$^-$ CD4$^+$ T cells after APC removal.

At sites of inflammation and immune activation, there is a correlation between CD4$^+$ trogocytosis and a heightened activation state (43). This is consistent with data showing that highly activated cells display enhanced trogocytic activity (4, 29). An additional explanation for the heightened activation observed in trogocytosis-positive (trog$^+$) cells is that that trogocytosed molecules could engage their receptors on the trog$^+$ CD4$^+$ T cell and sustain intracellular signaling. Such trogocytosis-mediated signaling may be playing an important and unappreciated role in driving and/or maintaining T cell activation, effector functions,

and differentiation. We have previously shown that that after APC removal, there is selective survival of trog^{+} cells over 5 days *in vitro* compared to trog^{-} cells (10). In addition, both TCR-proximal (ZAP-70 phosphorylation) and distal signaling (ERK 1/2 phosphorylation) was detectable in trog^{+}, but not trog^{-} cells 72 hours after APC removal. This sustained-signaling occurred independently of APC, and was driven by the engagement of trogocytosed molecules and their receptors on T cells (i.e. trogocytosis-mediated signaling) (10).

To extend on our previous study, we began by comparing the activation state and TCR-proximal signaling in trog^{+} and trog^{-} cells up to 72 hours after recovery from a 90-minute *in vitro* trogocytosis assay. Recovered T cells were analyzed immediately, or cultured for 3 days at low density (10^{4} cells/ml) to minimize T:T interactions, and samples were collected daily. At indicated time-points (Fig. 1), cells were analyzed via flow cytometry, and trog^{+} cells were identified by the presence of trogocytosed, biotin-labeled APC-derived molecules (Fig. S1C). Consistent with our previous findings, both trog^{+} and trog^{-} cells showed similar levels of TCR downmodulation immediately after the trogocytosis-assay, indicating that both populations had recognized antigen (Fig. 1A, B). In agreement with the TCR downmodulation data, both trog^{+} and trog^{-} cells also displayed elevated levels of the activation marker CD69, compared to unstimulated cells (Figs. 1C-E). However, after APC were removed from the system, only the trog^{+} cells maintained TCR downmodulation and an activated (CD69^{High}) phenotype throughout the 72-hour incubation. In contrast, at the 48 and 72-hour time points, the trog^{-} cells displayed significantly lower TCR downmodulation levels compared to the trog^{+} cells (Fig. 1B), and surface TCR levels were similar to unstimulated T cell blasts (Figs. 1A, B). The loss of TCR downmodulation coincided with a decrease in CD69 expression by the trog^{-} cells to levels similar to unstimulated T cell blasts (Figs. 1C, D), and at the 48 and 72-hour time points, the trog^{+} cells displayed significantly increased levels of CD69 compared to trog^{-} cells (Fig. 1D). This marked difference was not only due to the loss of CD69 expression by trog^{-} cells, but also a result of trog^{+} cells enhancing CD69 expression, and the loss of CD69^{Low} trog^{+} cells (Figs. 1C-E). In agreement with our previous study (10), the trog^{+} cells displayed enhanced survival compared the trog^{-} cells, as seen by the increase in trog^{+} frequencies, and decrease in trog^{-} frequencies after APC removal (Fig. 1C). While the phenotype of the trog^{+} cells is consistent with active-TCR signaling, the phenotype displayed by the trog^{-} cells is consistent with published data showing that CD69 expression peaks between 18–48 hours after removal of *in vitro* TCR stimulation (68).

To confirm that the TCR engagement displayed by trog^{+} cells resulted in TCR-proximal signaling, the levels of phosphorylated ZAP-70 (pZAP-70) were assessed (69, 70). In support of the data in Figs. 1A and B, and consistent with our previous studies (10), the trog^{+}, but not trog^{-} cells, maintained pZAP-70 levels after APC removal (Fig. 1E). At each observed time-point, the trog^{+} cells had significantly higher levels of pZAP-70, as determined by MFI, compared to the trog^{-} cells (Fig. 1F). Because nearly no APC were present in the cultures of CD4^{+} T cells following the trogocytosis-assay (Fig. S1B), the increased CD69 expression, TCR downmodulation, and elevated pZAP-70 maintained in trog^{+}, but not trog^{-}, cells over the 72-hour incubation suggests that cell-autonomous, trogocytosis-mediated signaling sustained the T cell activation.

Trog$^+$ CD4$^+$ T cells express elevated levels of IL-4 and IL-5, whereas trog$^-$ cells express high levels of IFNγ$^+$ and little IL-4 or IL-5.

The sustained activation and TCR proximal signaling in trog$^+$ cells after removal from APC raised the possibility that trogocytosis-mediated signaling may impact effector cytokine production within these cells. To examine this, culture supernatants from T cells recovered from the trogocytosis assay were analyzed for cytokines characteristic of various T_H subsets using cytokine-capture beads. Five hours after recovery from the *in vitro* trogocytosis-assay, T cell supernatants contained high levels of IFNγ and IL-2, but negligible amounts of IL-4, IL-6, IL-21 or IL-13 (Fig. 2A). Interestingly, by 72 hours IFNγ levels were significantly decreased, while IL-4 levels had increased significantly (Fig. 2A). To examine a potential correlation between trogocytosis and the observed cytokine production, intracellular cytokine staining (ICS) was performed on recovered cells at 24-hour intervals over a 72-hour incubation after APC removal. The fold-difference in MFI for T_H subset-characteristic cytokine expression of trog$^+$ and trog$^-$ cells compared to T cell blasts which did not undergo the trogocytosis-assay (unstimulated cells) is shown in Fig. 2B. Five hours post-recovery, neither the trog$^+$ nor trog$^-$ cells showed increased levels of IL-4, IL-5, IL-12, IL-6, IL-9, or IL-17, and the only cytokine showing substantially increased expression compared to unstimulated controls was IFNγ (Fig. 2B). Interestingly, at 5 hours IFNγ levels were increased in the trog$^-$ cells significantly more than in the trog$^+$ cells (Fig. 2D). By 72 hours, there were still minimal expression of IL-12, IL-6, IL-9, or IL-17 by both populations. The robust IFNγ expression seen in trog$^-$ cells at 5 hours was no longer apparent and had decreased to levels only marginally higher than that of unstimulated cells, while IFNγ levels remained minimal in trog$^+$ cells. However, the trog$^+$ cells had developed a striking 2.2-fold increase for IL-4 and 1.85-fold increase for IL-5, and 0.89-fold increase for IL-2, all of which were found to be significantly higher in the trog$^+$ cells compared to the trog$^-$ cells (Fig. 2B). Representative histograms for IFNγ and IL-4 expression by trog$^+$, trog$^-$, and unstimulated cells are presented in Fig. 2C. Enhanced IL-4 expression was also observed in trog$^+$ cells from parallel experiments using MCC peptide-pulsed BMDCs as APC (Fig. S2). Because the only significant differences in subset-characteristic cytokines detected between trog$^+$ and trog$^-$ cells were T_H1 and T_H2-associated, the subsequent experiments focused on these subsets.

Further assessment of the IFNγ and IL-4 production on a per-cell basis showed that the frequency of IL-4$^+$ cells increased exclusively in the trog$^+$ cells, from an average of 12.5% at 5 hours to an average of 73% by 72 hours (Fig. 2D). By comparison, the frequency of trog$^-$ IL-4$^+$ cells remained below 5% at all time-points. This resulted in significantly more trog$^+$ IL-4$^+$ cells than trog$^-$ IL-4$^+$ cells at 24, 48, and 72 hours (Fig. 2D *left*). In contrast, on average, 34% of the trog$^-$ cells, but only 10% of trog$^+$ cells were IFNγ$^+$ at 5 hours. Unlike IL-4, IFNγ expression was not maintained in trog$^+$ cells. Despite a dramatic loss of trog$^-$ IFNγ$^+$ cells, there was still a significantly lower frequency of trog$^+$ IFNγ$^+$ cells compared to the trog$^-$ IFNγ$^+$ cells at each observed time-point (Fig. 2D *right*). The decrease in trog$^-$ IFNγ$^+$ cells over the 72-hour incubation correlates with the loss of TCR signaling and activation seen in Fig.1, and the massive cell death in this population as observed in Fig. 1C and our previous study (10).

The strong IFNγ^+ expression in trog$^-$ cells at 5 hours further demonstrates that both trog$^+$ and trog$^-$ cells are fully activated by the initial APC encounter. Thus, differences in the phenotype between trog$^+$ and trog$^-$ cells do not simply reflect whether T cells have recognized Ag. In addition, although trog$^+$ cells displayed sustained signaling and activation (Fig. 1), IFNγ expression in these cells was not maintained. Combined with the increase in IL-4 expression by trog$^+$ cells after removal from APC, these results are consistent with the possibility that trogocytosis-mediated signaling was impacting the effector cytokine production of the trog$^+$ cells, in a manner consistent with a T_H2 phenotype.

T_H2 cells are more efficient than T_H1 or non-polarized CD4$^+$ T cells at performing trogocytosis.

One potential explanation for the increased IL-4 expression and frequency observed in trog$^+$ cells is that pre-T_H2 or T_H2-like cells had performed trogocytosis more efficiently than pre-T_H1 / T_H1-like cells. Thus, the increase in IL-4$^+$ trog$^+$ cells may simply reflect the superior survival displayed by trog$^+$ cells after removal from APC (10). To compare the trogocytic potential of differentiated T_H1 and T_H2 cells, *in vitro*-polarized T_H1 and T_H2 blasts were used in an *in vitro* trogocytosis assay (Figs. 3A, B). Representative histograms in Fig. 3C and D show that GATA-3$^+$ T_H2 blasts were highly efficient at performing trogocytosis, with an average of 71.5% displaying biotin-labeled APC-membrane and 58.1% having I-E^k on their surface. In contrast, T-bet$^+$ T_H1 cells were weakly trogocytic, averaging only 14.2% of cells with detectable APC-membrane and 10.4% being I-E^{k+}. For comparison, non-polarized blasts, which showed a predominant T_H1 phenotype (Figs. 3A, B), averaged 26.8% of cells with detectable APC-membrane, and 16.8% with trogocytosed I-E^k. Thus, while non-polarized cells had a significantly higher frequency of trog$^+$ cells compared to polarized T_H1 cells, the T_H2 cells performed trogocytosis at significantly higher rates than both non-polarized, and T_H1 cells (Fig. 3E). These results support the hypothesis that the predominant T_H2-associated cytokine production in the trog$^+$ cells at 72 hours (Fig. 2) was, at least in part, due to the increased ability of T_H2 cells to perform trogocytosis and their subsequent enhanced survival, which was driven by trogocytosis-mediated signaling.

Trogocytosis-mediated signaling is sufficient, and effective, in driving IL-4 expression.

Based on the data in Fig. 3 showing that T_H2 cells possess higher trogocytic potential than T_H1 or non-polarized cells, the increase in trog$^+$ IL-4$^+$ cells may simply be due to trogocytosis-mediated signaling enhancing the survival of predestined T_H2 cells. If this were the case, then sustained-canonical TCR and costimulatory signaling would be expected to augment the T_H2 phenotype of pre-T_H2 or T_H2 cells. To examine this possibility, an aliquot of the same T cell blasts to be used in a trogocytosis-assay were stimulated with plate-bound anti-CD3 + anti-CD28 in parallel with T cells recovered from a standard *in vitro* trogocytosis-assay. At 72 hours, on average, 77.4% of the trog$^+$ cells were IL-4$^+$, but only 3.5% of trog$^-$ cells and 1.8% of Ab-stimulated blasts were IL-4$^+$ (Figs. 4A-C). In contrast, Ab-stimulated blasts maintained a similar frequency of IFNγ^+ cells over the 72 hours (Fig. 4A), while the frequency of IFNγ^+ trog$^+$ cells dropped from an average of 13.4% at 5 hours to 1.5% by 72 hours (Fig. 4C). The striking difference between the IFNγ and IL-4 expression patterns between the trog$^+$ and Ab-stimulated blasts suggests that trogocytosis-mediated signaling provides additional, potentially unique, signals that favor T_H2-associated

cytokine expression, beyond the signaling induced by repeated CD3 + CD28 signaling. These results further strengthen the association between trogocytosis-mediated signaling, and a T_H2 phenotype.

As seen in Fig. 3, the majority of non-polarized T cells did not displayed a T_H1 phenotype prior to the trogocytosis assay, yet the vast majority of $trog^+$ cells developed a T_H2 phenotype after APC removal. While the data thus far is suggestive that trogocytosis-mediated signaling was driving this phenotype, the possibility that residual signaling from the T:APC interaction was driving the observed IL-4 expression in $trog^+$ cells remained. To confirm that trogocytosis-mediated signaling alone was capable of driving IL-4 production in $trog^+$ cells, Lck signaling was interrupted in cells recovered from the trogocytosis assay with the reversible Src family kinase inhibitor PP2. Using this technique, we previously demonstrated that PP2 treatment terminated TCR signaling, however, after removal of PP2, signaling was re-initiated in $trog^+$, but not $trog^-$ cells (10). Here, we hypothesized that if trogocytosis-mediated signaling was driving IL-4 expression, then cytokine production would resume in $trog^+$, but not $trog^-$ cells after removal of PP2. If neither $trog^+$ nor $trog^-$ cells re-initiated IL-4 expression after PP2 was removed, it would indicate that trogocytosis-mediated signaling alone was insufficient to drive the expression of IL-4. Immediately following the trogocytosis assay, recovered cells were treated for 20 min with PP2 to halt TCR signaling, and then incubated for an additional 2 hours after PP2 removal. Results in Fig. 4D show that PP2 treatment did not alter the engagement of TCR by trogocytosed MHC:peptide complexes, as nearly identical levels of TCR downmodulation were observed in PP2-treated $trog^+$ and untreated $trog^+$ cells, at 2 (MFI reduced 2.9 fold or 2.81 fold vs. unstimulated controls, respectively) and 72 hours (1.7 fold vs. 1.3 fold reduction, respectively) (Fig. 4D). Treatment with PP2 did however, reduce the frequencies of $trog^+$ $IL\text{-}4^+$ cells at 2 hours by an average of 83.5% (from 11% to 1%). However, 72 hours after PP2 removal, the frequency of $IL\text{-}4^+$ $trog^+$ cells had rebounded from 1% at 2 hours, to nearly 60% at 72 hours (Fig. 4D, *right*). PP2 treatment also decreased the modest IL-4 expression of $trog^-$ cells at 2 hours, and, as expected, neither the PP2-treated or untreated populations of $trog^-$ cells expressed IL-4 at 72 hours (Fig. S3C). The ability of $trog^+$ cells to resume IL-4 production in absence of APC provides compelling evidence that trogocytosis-mediated signaling was sufficient to drive IL-4 expression in $trog^+$ cells.

Treatment with PP2 reduced the frequency of $trog^+$ $IFN\gamma^+$ cells by 72%, and $trog^-$ $IFN\gamma^+$ cells by 80% at 2 hours (Fig. S3). However, consistent with the hypothesis that trogocytosis-mediated signaling was driving IL-4, but not IFNγ expression, the expression of IL-4, had rebounded in $trog^+$ cells 24 hours after PP2 treatment, while IFNγ expression was significantly lower in PP2-treated cells compared to untreated cells (Fig. 4E). This suggests that IFNγ expression was due to signaling occurring at the immunological synapse, and that trogocytosis-mediated signaling was insufficient to maintain IFNγ production in these cells.

Intracellular IL-4 is polarized towards trogocytosed molecules

The sustained expression of IL-4 by $trog^+$ cells up to 72 hours after removal from APC (Fig. 2) suggested that trogocytosis-mediated signaling may be contributing to the maintenance of T_H2-associated cytokine production in these cells. As a major function of T_H2 cells is to

provide contact-dependent help to cognate B cells upon Ag recognition through B cell directed cytokine secretion, we hypothesized that trogocytosis-mediated signaling may mimic these T:B interactions. If so, intracellular IL-4 would likely be polarized towards areas of trogocytosis-mediated TCR-signaling. Three days after recovery from a standard *in vitro* trogocytosis assay, recovered cells were stained for trogocytosed molecules, intracellular IL-4, and pZAP-70, and analyzed by confocal microscopy. Consistent with the flow-cytometry data (Fig. 2), IL-4 was only detected in 5% of trog$^-$ cells in which polarization of IL-4 towards any distinct region was only observed in 8% of trog$^-$ IL-4$^+$ cells (Figs. 5C, S4). In contrast, the trog$^+$ IL-4$^+$ cells had significantly higher frequencies of polarized IL-4 compared to the trog$^-$ IL-4$^+$ cells, and 86% of these cells had IL-4 polarized towards trogocytosed molecules on the T cell membrane (Fig. 5C). Representative images illustrate that IL-4 was polarized towards trogocytosed molecules (Fig. 5A), and that proximal TCR-signaling was occurring at the trogocytosed molecules, as indicated by pZAP-70 staining (Fig. 5B). Additional images are presented in Fig. S4. These images are reminiscent of observations made by Kupfer *et al.*, who revealed that during T_H2 help for B cells, IL-4 delivery was localized to the T_H2:B cell interface (71). Thus, data in Fig. 5 are supportive of a model where trogocytosis-mediated signaling was stimulating polarized IL-4 secretion, and also further reinforce the T_H2 phenotype displayed by trog$^+$ cells.

Trog$^+$ cells develop a T_H2 phenotype while trog$^-$ cells maintain a T_H1 phenotype after separation from APC.

Although IL-4 is widely accepted as the representative T_H2 effector-cytokine, other T cell subsets, such as T_{FH}, also express IL-4 (72). Therefore, expression of IL-4 alone does not indicate T_H2-differentiation. To determine whether trog$^+$ cells were differentiated to T_H2, the expression of subset-characteristic transcription factors was examined. The data in Fig. 6A show no detectable differences in expression of GATA-3 (T_H2), T-bet (T_H1), Foxp3 (T_{reg}), Bcl-6 (T_{FH}) or RORγt (T_H17) between trog$^+$ and trog$^-$ cells, 5 hours post-recovery from an *in vitro* trogocytosis-assay. This further supported that the unstimulated blasts consisted of a homogenous population prior to use in the trogocytosis-assay. By 72 hours however, the trog$^+$ cells displayed a 1.7-fold increase for GATA-3, and 90% lower levels of T-bet compared to trog$^-$ cells, while only minimal differences were detected for Foxp3, Bcl-6, or RORγt (Fig. 6A). In agreement with the cytokine profiles observed in Fig. 2, over the 72-hour incubation, T-bet expression in trog$^+$ cells decreased to a level below unstimulated bulk T cell blasts, while trog$^-$ cells maintained elevated T-bet expression (Fig. 6B). In contrast, at 72 hours, the majority of the trog$^+$ cells were GATA-3$^+$, and GATA-3 expression was negligible in the trog$^-$ cell population (Fig. 6B). While trog$^+$ and trog$^-$ displayed similar levels of T-bet and GATA-3 five hours after recovery, by 72 hours the trog$^+$ cells displayed significantly increased GATA-3 expression, and significantly decreased T-bet expression compared to trog$^-$ cells (Fig. 6C). These results confirmed that the IL-4$^+$ trog$^+$ cells were consistent with a T_H2 phenotype, and support the hypothesis that trogocytosis-mediated signaling was driving T_H2 differentiation rather than simply enhancing the survival of T_H2-commited cells.

Trogocytosis-mediated signaling, rather than IL-4 availability, is required for GATA-3 upregulation after APC removal.

While IL-4 is a major product of T_H2 cells, it is also an inducer of this subset, as IL-4R-signaling significantly contributes to T_H2 differentiation (73). Because the trog$^+$ cells produced significantly higher amounts of IL-4 than trog$^-$ cells (Fig. 2), it was possible that the T_H2 phenotype displayed by the trog$^+$ cells was simply the result of IL-4 availability. To examine whether IL-4R signaling was playing the central role in the T_H2-phenotype observed in trog$^+$ cells, exogenous IL-4 (20 μg/ml) was added to cultures of cells immediately after recovery from the trogocytosis-assay, and replenished at 24 hours. As seen in Fig. 6D, at 72 hours, the addition of IL-4 had minimal effects on GATA-3 expression in unstimulated cells. Similarly, the trog$^-$ cells from cultures containing supplemented IL-4, showed only an 8.6% average increase in GATA-3 expression, while trog$^+$ cells from the same cultures had increased GATA-3 expression by an average of 25.5%, as determined by MFI (Fig. 6E). However, the addition of IL-4 had little impact on the frequency of GATA-3$^+$ trog$^-$ or trog$^+$ cells, as no significant differences between cells from untreated cultures, and cultures with supplemented IL-4, were detected in either population (Fig. 6F). Thus, IL-4R signaling was not playing the central role in the increase in GATA-3$^+$ expression by the trog$^+$ cells. These results confirm that trogocytosis-mediated signaling, and not simply the availability of IL-4, was essential for the observed T_H2 phenotype developed in trog$^+$ cells, consistent with the finding that GATA-3 translation is dependent on TCR signaling (74).

Trogocytosis-mediated signaling drives T_H1 cells to express IL-4 and GATA-3

The results in Figs. 4 and 6 are consistent with the hypothesis that trogocytosis-mediated signaling drives T_H2 differentiation in trog$^+$ cells. To examine this hypothesis, we tested whether trogocytosis-mediated signaling could induce *in vitro* T_H1 polarized trog$^+$ cells to start producing T_H2 characteristic proteins. If such conversion was observed in trog$^+$, but not trog$^-$, polarized T_H1 cells it would strongly support the hypothesis that sustained, trogocytosis-mediated signaling was inducing a T_H2 phenotype. *In vitro* T_H1 and T_H2 polarized blasts were generated and used in a standard *in vitro* trogocytosis assay. In parallel, polarized T_H1 and T_H2 blasts were stimulated on anti-CD3 + anti-CD28 coated plates to provide sustained signaling throughout the 72-hour incubation. Because plasticity between T_H1 and T_H2 subsets occurs only after days of exposure to alternate polarizing conditions (75–78), the 90 minutes of exposure to APC during the trogocytosis-assay alone would not likely be sufficient to induce T_H1 to T_H2 conversion. Cells were examined at 5 hours to examine baseline conditions, and at 72 hours after APC removal, to assess potential phenotypic changes.

The results in Fig. 7A show that sustained Ab-stimulation resulted in stable IFNγ expression in polarized T_H1 cells, with an average of 61% being IFNγ$^+$ at 5 hours, and 57% being IFNγ$^+$ at 72 hours. As anticipated, these T_H1 polarized cells did not express IL-4 at any time-point. The T_H1 polarized trog$^+$ cells showed a phenotype similar to Ab-stimulated T_H1 cells at 5 hours, with an average of 79% being IFNγ$^+$, and only 8% expressing IL-4$^+$ (Fig. 7B). However, unlike the Ab-stimulated T_H1 cells, the frequency of trog$^+$ IFNγ$^+$ cells decreased at each successive time-point, and by 72 hours only ~5% remained IFNγ$^+$. IFNγ

expression was not detected in the trog$^+$ T_H2, or the Ab-stimulated T_H2 blasts at any time-point (Figs. 7 C, D).

In contrast to the significant decrease in IFNγ expression, the frequency of trog$^+$ T_H1 polarized cells expressing IL-4 increased from 8% at 5 hours, to approximately 70% at 72 hours (Fig. 7B). The presence of a unique population (averaging 4.7%) of T_H1 polarized trog$^+$ cells which were IFNγ^+ IL-4$^+$ double-positive cells at 72 hours (Fig. 7B) supported the idea that these cells converted from T_H1 towards a T_H2 phenotype (79). For comparison, while Ab-stimulation of the polarized T_H1 maintained IFNγ expression, on average, less than 0.2% of these cells were for IFNγ^+ IL-4$^+$ double-positive at 72 hours (Fig. 7A). Within the polarized T_H2 cells, on average only 0.22% of trog$^+$, and 0.31% of Ab-stimulated cells were IFNγ^+ IL-4$^+$ (Fig. 7C, D).

While the T_H2 polarized trog$^+$ population displayed an average of 84.2% of cells being IL-4+, somewhat unexpectedly, only 28% of Ab-stimulated cells, were IL-4$^+$ at 72 hours (Fig. 7C, D). These are similar to the results in Fig. 4, and further support that trogocytosis-mediated signaling is favorable for driving and/or augmenting a T_H2 phenotype, while sustained anti-CD3 + anti-CD28 Ab-stimulation is not.

In addition to shutting down IFNγ expression and upregulating IL-4, the trog$^+$ T_H1 polarized cells also displayed a shift in transcription factor expression. These cells were GATA-3 negative and expressed high levels of T-bet at 5 hours, but by 72 hours, the trog$^+$ T_H1 cells had upregulated GATA-3 expression, and approximately half of the population lost T-bet expression (Fig. 7E). In contrast, the Ab-stimulated and trog$^-$ T_H1 cells remained GATA-3$^-$ and maintained expression of T-bet at 72 hours. While there were no significant differences in T-bet or GATA-3 expression between T_H1 polarized trog$^+$, trog$^-$, and Ab-stimulated cells 5 hours after recovery, by 72 hours the frequency of T-bet$^+$ cells was significantly lower in the trog$^+$ population compared to trog$^-$ population. This was concomitant with significantly more trog$^+$ cells expressing GATA-3 compared to trog$^-$ and Ab-stimulated cells (Fig. 7F). Consistent with the cytokine expression data where the T_H1 polarized trog$^+$ cells expressed both IL-4 and IFNγ (Figs. 7A, B), significantly more trog$^+$ cells also expressed both T-bet and GATA-3 compared to trog$^-$ and Ab-stimulated cells (Fig. 7F). Taken together, the data in figure 7 strongly suggests that trogocytosis-mediated signaling induced T_H1 to T_H2 conversion, strengthening the conclusion that trogocytosis-mediated signaling drove the observed T_H2 phenotype in trog$^+$ cells.

Trogocytosis$^+$ CD4$^+$ T cells generated *in vivo* display a T_H2 phenotype.

The results so far strongly support the hypothesis that trogocytosed molecules engage cognate receptors on T cells to sustain intracellular signaling, leading to T_H2 biasing. To examine whether this *in vitro* phenotype was consistent with *in vivo* immune responses, a protein immunization model in an adoptive transfer system, using TCR-transgenic T cells transferred into wild type animals was used, as well as the direct protein immunization of wild type animals. In the adoptive transfer model, B10.A mice were immunized subcutaneously with whole pigeon cytochrome-c (PCC) protein. Twenty-four hours later, naïve 5C.C7 TCR-transgenic T cells were adoptively transferred into the immunized animals (Fig. 8). Five days after the adoptive transfer, cells were harvested from draining lymph

nodes and analyzed. Of the recovered, adoptively transferred $CD4^+$ T cells, there was significantly higher rates of trogocytosis in the PCC-immunized animals (averaging 19.4% $trog^+$) compared PBS-injected controls (averaging 0.28% $trog^+$) (Fig. 8A). Based on CD69 upregulation and TCR downmodulation, both $trog^+$ and $trog^-$ adoptively transferred $CD4^+$ T cells had recognized Ag and were activated (Fig. 8B). Consistent with the *in vitro* results in Fig. 1, the $trog^+$ $CD4^+$ T cells showed trends of higher activation and TCR downmodulation compared to $trog^-$ $CD4^+$ T cells from the same animal (Fig. 8B). Within the activated ($CD69^{High}$) $CD4^+$ T cells, there was a significantly higher frequency of $trog^+$ IL-4^+ cells than $trog^-$ IL-4^+ cells (Fig. 8C). On average, 15% of $trog^-$ cells and 11% of $trog^+$ cells were IFNγ^+ (Fig. 8C), resembling the phenotypes observed at 48 hours following recovery from the *in vitro* trogocytosis-assay (Fig. 2D). Also, consistent with the phenotype of cells recovered from the *in* vitro trogocytosis assays (Fig. 2C), the expression of IL-4 on a per-cell basis, was higher in $trog^+$ cells than similarly activated $trog^-$ cells (Fig. 8D).

In a parallel set of experiments, non-transgenic C57BL/6 mice were immunized with chicken ovalbumin (OVA), followed by a booster immunization 14 days later. $CD4^+$ T cells were recovered from draining lymph nodes five days after the second immunization. These time-points were chosen to reintroduce antigen at the end of the effector stage of the immune response, but before establishment of a stable memory population. OVA immunized animals had significantly higher frequencies of $trog^+$ $CD4^+$ T cells compared to PBS-injected control mice (Fig. 8E). Consistent with our previous study (10), the $trog^+$ cells displayed sustained survival *ex vivo*, as the frequency of isolated $trog^+$ $CD4^+$ T cells from OVA-immunized mice increased from 8% on the day of harvest to nearly 60% after a five-day *in vitro* incubation (Fig. 8D). Similar to the results with the TCR-transgenic model, the $trog^+$ $CD4^+$ T cells were more activated than $trog^-$ $CD4^+$ T cells as determined by CD69 staining (Fig. 8F). Within the activated ($CD69^{High}$) $CD4^+$ cell populations, the $trog^+$ cells displayed increased expression of GATA-3 and IL-4, whereas their expression in $trog^-$ cells from the same animal was nearly identical to that of $CD4^+$ T cells recovered from PBS-control animals (Fig. 8F). Similar to results from *in vitro* and *in vivo* TCR-transgenic experiments (Figs. 2, 8C), the frequency of GATA-3^+ $CD4^+$ cells was significantly higher in the $trog^+$ cells compared to the $trog^-$ cells (Fig. 8G). Consistent with these results, of cells recovered from OVA-immunized mice, the frequency of IL-4^+ cells was significantly higher in $CD69^{High}$ $trog^+$ cells, at nearly 50%, compared to the $CD69^{High}$ $trog^-$ cells, of which 22.3% were IL-4^+. (Fig. 8H). Collectively, the results in Fig. 8 provide strong corroboration of the results obtained from the *in vitro* experiments, as $trog^+$ $CD4^+$ T cells generated *in vivo* displayed enhanced survival *in vitro*, and displayed greater activation, as well as increased GATA-3 and IL-4 expression, compared to $trog^-$ cells from the same animal. These results support the hypothesis that trogocytosis-mediated signaling may play a role in T_H2 differentiation *in vivo*.

Discussion

Trogocytosis by $CD4^+$ T cells results the presence of functional, APC-derived molecules, including MHC:peptide complexes, on the surface of the $trog^+$ T cell. Many of these acquired molecules are not expressed endogenously by the T cell, but they clearly have an impact on T cell biology. This has been demonstrated by the ability of $trog^+$ cells to impact

the activation of other T cells through the presentation of trogocytosed molecules (9, 15). We have found that trogocytosed molecules are also engaged by cognate receptors on the trog$^+$ T cell (10), however the biological implications of this phenomenon are largely unknown. Because trogocytosis commonly occurs during the activation of CD4$^+$ T cells, it is important to develop a comprehensive understanding of the biological consequences of this event.

In this study, we examined the impact of sustained, trogocytosis-mediated signaling on the activation, effector cytokine production, and differentiation of the trog$^+$ T cell. Trog$^+$ cells have sustained TCR proximal signaling for at least 72 hours after APC removal, consistent with cell-autonomous signaling resulting from engagement of the receptors on the T cell by trogocytosed molecules (Fig. 1). This sustained signaling was not due to T:T presentation or the presence of contaminating APC, as only the trog$^+$ cells maintained a phenotype consistent with active TCR signaling and sustained activation, despite the cultures containing both trog$^+$ and trog$^-$ cells throughout the incubation period. This conclusion is further supported by images showing that active TCR signaling occurred proximal to trogocytosed molecules on the surface of trog$^+$ cells, 72 hours after removal from APC (Fig. 5). Similar to our previous studies, the sustained signaling led to preferential survival of the trog$^+$ cells, as the frequency of CD4$^+$ cells that were trog$^+$ increased from roughly 25% immediately after recovery from the trogocytosis-assay, to nearly 80% 72 hours later (Fig. 1C, (10).

Because the trog$^+$ cells had sustained TCR signaling and remained activated 72 hours after APC removal, we investigated whether trogocytosis-mediated signaling might impact the effector cytokine production of these cells. Intracellular cytokine staining of cells 5 hours after recovery from the trogocytosis-assay showed that a significantly higher frequency of trog$^-$ cells were IFNγ^+ compared to trog$^+$ cells. However, IFNγ levels decreased to resting levels in both trog$^-$ and trog$^+$ cells over a subsequent 72-hour incubation (Fig. 2B, C). While the frequency of trog$^-$ IL-4$^+$ cells remained at approximately 5% over the 72-hour incubation, the average frequency of trog$^+$ IL-4$^+$ cells increased from 10% at 5 hours, to over 70% at 72 hours (Fig. 2D). Because the trog$^+$ cells also displayed enhanced survival after APC removal (Fig. 1C), the trog$^+$ cells accounted for over 98% of the total IL-4$^+$ CD4$^+$ cells at 72 hours. The increase in the frequency of trog$^+$ IL-4$^+$ cells over the 72-hour incubation was likely not due to increased proliferation of the trog$^+$ cells, as the amount of trogocytosed molecules on the trog$^+$ cells remained constant and was not diluted, as would be expected for dividing cells. In addition, our previous study showed no discernable proliferation of trog$^+$ cells up to 5 days after removal from APC (10). These results are consistent with the observations that trogocytosed molecules are retained in a punctate spot on the membrane of the trog$^+$ cell (Fig. 4, (4, 10). Thus, the data suggests that trogocytosis-mediated signaling led to sustained survival of IL-4$^+$ cells, and/or directly impacted the IL-4 expression in the trog$^+$ cells.

If the trogocytosis-mediated signaling was simply sustaining the survival of IL-4-expressing cells, the apparent increase in IL-4$^+$ trog$^+$ cells after APC removal might be due to a difference in the ability of T_H1 and T_H2 cells to perform trogocytosis. We found that when *in vitro* polarized T_H1 and T_H2 cells and non-polarized T cells were compared, the T_H2 polarized cells were indeed more efficient at performing trogocytosis (Fig. 3). However, the

difference in the efficiency of trogocytosis alone isn't sufficient to account for the observed phenotypes. While the frequency of trog$^+$ IL-4$^+$ cells increased, the frequency of trog$^+$ IFNγ producing cells decreased from 10% at 5 hours after recovery to 0.5% at 72 hours, suggesting that trogocytosis-mediated signaling was not simply boosting global intracellular signaling and enhancing the survival of all trog$^+$ cells. If that were the case, the frequency of IFNγ-expressing and IL-4-expressing cells would be expected to remain relatively stable. Rather, our results suggested that trog$^+$ cells were differentiating into T_H2 (GATA-3$^+$ IL-4$^+$) cells after the trogocytosis-assay. While robust GATA-3 expression was detected in trog$^+$ cells by 72 hours (Fig. 6), anti-CD3 + anti-CD28 stimulation of an aliquot of the unstimulated T cell blasts used in the trogocytosis-assay did not result in a similar T_H2 phenotype (Fig. 4A). Furthermore, T cell blasts immediately prior to the trogocytosis assay displayed a relatively homogeneous T_H0/T_H1 phenotype (Figs. 2, 3, 6). This is consistent with the inherent bias towards a T_H1 phenotype possessed by the 5C.C7 TCR transgenic mice used in our experiments (80, 81), and may explain the rapid IFNγ production, and delay in IL-4 expression, observed in the cells after recovery from the trogocytosis-assay.

To eliminate the possibility that the observed IL-4 production in the trog$^+$ cells was induced by residual signaling received from the T:APC interaction and directly examine the role of trogocytosis-mediated signaling in the observed T_H2 phenotype of trog$^+$ cells, the reversible Lck inhibitor PP2 was used to halt TCR signaling after APC removal, then washed out to allow trogocytosis-mediated signaling to resume. We found that after PP2 removal, IFNγ expression did not resume in either trog$^+$ or trog$^-$ cells (Figs. 4D, 4E, S3), consistent with IFNγ production being induced by interactions with APC, and not induced further by trogocytosis-mediated signaling. In contrast to IFNγ, the frequency of trog$^+$ IL-4$^+$ cells from PP2-treated cultures rebounded to levels equal to untreated cells by 24 hours after PP2 removal (Fig. 4E), and robust IL-4 production was observed in trog$^+$ cells 72 hours after PP2 treatment (Figs. 4B, C). These significant findings show that trogocytosis-mediated signaling was sufficient to drive IL-4 expression in trog$^+$ cells. The results showing that *in vitro* T_H1 polarized trog$^+$ cells began expressing IL-4 and GATA-3, while at the same time decreasing expression of IFNγ and T-bet (Fig. 7), further support that, at least in absence of external stimuli, trogocytosis-mediated signaling promotes T_H2 differentiation. Although it is possible that a portion of the trog$^+$ blasts generated under T_H1-polarizing conditions were not fully differentiated to T_H1 prior to use in the trogocytosis assay, the unique population of double-positive cells expressing both IFNγ and IL-4 (Fig. 7B), and the transcription factors T-bet and GATA-3 (Fig. 7F), was only apparent within the trog$^+$ cells generated under T_H1-polarizing conditions. Thus, the data in Fig. 7 supports the possibility that trogocytosis-mediated signaling is capable of inducing T_H1 to T_H2 conversion. That a greater frequency of T_H2 polarized trog$^+$ cells produced IL-4 than Ab-stimulated T_H2 polarized cells at 72 hours (Fig. 7C, D), further supports the hypothesis that trogocytosis-mediated signaling is potent in driving IL-4 expression. Taken together, the data presented here is consistent with the concept that trogocytosis-mediated signaling can drive the differentiation of CD4$^+$ T cells towards a T_H2 phenotype.

The T_H2 phenotype observed *in vitro* with trog$^+$ cells was also apparent in *in vivo* immune responses. Using TCR-transgenic or wild type cells, and with different antigen systems, we observed that *in vivo* derived CD4$^+$ trog$^+$ cells expressed IL-4 and GATA-3 at greater levels,

and higher cell frequencies, compared to trog$^-$ cells from the same animal (Fig. 8B, C). The observed T_H2 phenotype of *in vivo* trog$^+$ cells was less robust than the phenotype developed in *in vitro* assays, however, this is consistent with findings that in some cases, GATA-3 expression in T_H2 CD4$^+$ T cells is less pronounced in *in vivo* than *in vitro* (82). The observed phenotype may also be attributed to the inherent nature of the mice used in our study towards T_H1, which, consequently, further underscores the significance of the T_H2 phenotype developed by trog$^+$ cells in this study. Further studies are underway to characterize the T_H2 phenotype of *in vivo*-generated trog$^+$ cells at additional time-points, and after immunization with T_H1-inducing components.

It is interesting to speculate on the mechanisms leading to the observed association between CD4$^+$ trog$^+$ cells and a T_H2 phenotype. It has been found that the strength, duration, and "summation" of TCR and costimulatory molecule signaling can substantially impact T helper differentiation (82–85). In non-differentiated cells, it is possible that immune synapses that result in trogocytosis may be of shorter duration and/or generate weaker TCR signaling. This would be consistent with observations that weaker TCR signaling drives early IL-4 production by T cells (84, 86–88). Because only a fraction of the APC molecules involved in the immunological synapse are transferred to the T cell, trogocytosis-mediated signaling is likely weaker than signaling at the synapse. This signaling could further promote IL-4 production, consistent with the increased levels of IL-4 observed in trog$^+$ cells over a 72-hour incubation (Figs. 2, 4, 7). The T_H1 to T_H2 conversion observed with T_H1 polarized trog$^+$ cells (Fig. 7) further supports this model, as weak TCR-signaling drives T_H2 differentiation, even under T_H1- polarizing conditions (89). In contrast, IFNγ production and T_H1 differentiation have been shown to require strong TCR-signaling (90–92).

The differences in trogocytosis efficiency between polarized T_H1 and T_H2 cells may also be attributed to morphological differences in the immunological synapse formed. We have previously shown that at low Ag concentrations, T_H1 synapses form the classical "bull's-eye" shape, while T_H2 cells form multi-focal synapses (66). In separate live-cell imaging experiments, we have observed that small "packets" of MHC:peptide are transferred from APC to non-polarized T cells from the immunological synapse, before becoming localized to a punctate spot at the distal pole of the T cell membrane (93). It is inviting to speculate that the multi-focal synapses formed by T_H2 cells facilitate trogocytosis much more efficiently than the synapses formed by T_H1 cells, although that was not directly tested here.

There are many biological implications of trogocytosis-mediated signaling driving and/or augmenting a T_H2 phenotype, while also antagonizing a T_H1 phenotype. Such implications are amplified when considering that trog$^+$ cells display sustained survival, along with enhanced activation and effector cytokine production (Figs. 1, 2, (10)). The T_H2 phenotype itself may contribute to the enhanced survival displayed by trog$^+$ cells (Fig. 2C, (10)), as IL-4 has been found to enhance CD4$^+$ survival both *in vitro* and *in vivo* (94). Additionally, a T_H2 phenotype may aid in the heightened activation commonly observed in trog$^+$ cells, as T_H2, but not T_H1 cells, have been shown to be able to revert from an anergic state to resume effector functionality (95). It is possible that trog$^+$ T_H2 cells may significantly aid in the generation of B cell germinal centers, and/or increase the quality and duration of protective antibody generation when Ag is limited. On the other hand, the low trogocytic potential of

T_H1 cells, and the T_H2 phenotype induced by trogocytosis-mediated signaling, could act as checkpoint to limit unwanted T_H1-associated inflammation after Ag clearance.

In cases where a T_H2 response is undesirable, excessive $CD4^+$ trogocytosis may play a role in exacerbating T_H2-mediated autoimmune diseases such as SLE and rheumatoid arthritis, heighten allergic reactions, or negatively impact protective cell-mediated responses. In a study by Brown *et al.*, $CD4^+$ T cells from patients with multiple myeloma showed increased rates of trogocytosis and the $trog^+$ cells displayed inhibitory effects on proliferation of stimulated T cells (34). The authors proposed that trogocytosis might play a role in tumor-induced immune suppression through T-cell fratricide and deletion in patients with multiple myeloma. It is possible that in tumor environments where antigen is presumably abundant, a high frequency of $CD4^+$ trogocytosis and subsequent T_H2-differentiation/conversion could significantly suppress an anti-tumor response. Such suppression may be attributed to the inhibition of anti-tumor promoting T_H1 cell differentiation by trogocytosis-mediated signaling, and the high IL-4 production by $trog^+$ cells, as IL-4 has been shown to both inhibit IFNγ production and prevent activation of naïve T cells (96).

Beyond driving a T_H2 phenotype, continual trogocytosis-mediated signaling may aid in the generation of $CD4^+$ memory and/or T_{FH} cells, as both subsets require sustained-TCR signaling through repeated Ag-encounter for their differentiation (82, 97). As T_H2 to T_{FH} conversion has been found to take between 5 to 7 days to occur *in vivo* (98), examining the phenotype of $trog^+$ cells at extended time-points is likely necessary to determine this possibility. Studies are currently underway in our lab to examine the potential role of trogocytosis-mediated signaling in the generation of both T_{FH} and memory $CD4^+$ T cells.

In conclusion, the results from this study provide further insight into the role of trogocytosis and trogocytosis-mediated signaling in the activation, effector cytokine production and differentiation of $CD4^+$ T cells. We report a strong association between $CD4^+$ trogocytosis and a T_H2 phenotype, which is twofold, as T_H2 cells are highly efficient at performing trogocytosis, while trogocytosis-mediated signaling induced T_H2 differentiation in both non-polarized, and polarized T_H1 cells. We propose a model for trogocytosis-mediated $CD4^+$ differentiation in which trogocytosed MHC:peptide complexes and costimulatory molecules sustain intracellular signaling by engaging their cognate receptors on the $trog^+$ T cell. The relatively weak intensity of this signaling leads to early IL-4 production, which is sustained by trogocytosis-mediated signaling. In the presence of IL-4, the sustained trogocytosis-mediated TCR-signaling drives GATA-3 expression, and thus, T_H2 differentiation (74). Because $trog^+$ $CD4^+$ possess the unique ability to remain activated independently of further APC encounter via trogocytosis-mediated signaling, results from this study raise the possibility that $CD4^+$ trogocytosis may play a role in augmenting, or inducing a T_H2-dominant immune response.

Supplementary Material

Refer to Web version on PubMed Central for supplementary material.

Acknowledgments

We thank the University of Montana Fluorescence Cytometry core and the core staff scientist Pam Shaw, for expert technical assistance with flow cytometry. We also thank Dr. Jay Evans, and Dr. Alyson Smith and Center for Translational Medicine for the use of their LSRII and for helpful discussions. In addition, we thank the University of Montana Molecular Histology and Fluorescence Imaging Core and the core staff scientist Lou Herritt for expertise and technical assistance with imaging experiments. Finally, we would like to thank Dawit Mengistu, Morgan Stark, Dr. Shannon Miller, and Dr. Mike Minnick for critical review of the manuscript.

References

1. Hudrisier D, Riond J, Mazarguil H, Gairin JE, and Joly E. 2001 CTLs rapidly capture membrane fragments from target cells in a TCR signaling-dependent manner. J Immunol 166: 3645–3649. [PubMed: 11238601]
2. Joly E, and Hudrisier D. 2003 What is trogocytosis and what is its purpose? Nat Immunol 4: 815. [PubMed: 12942076]
3. Baba E, Takahashi Y, Lichtenfeld J, Tanaka R, Yoshida A, Sugamura K, Yamamoto N, and Tanaka Y. 2001 Functional $CD4^+$ T cells after intercellular molecular transfer of 0X40 ligand. J Immunol 167: 875–883. [PubMed: 11441094]
4. Wetzel SA, McKeithan TW, and Parker DC. 2005 Peptide-specific intercellular transfer of MHC class II to $CD4^+$ T cells directly from the immunological synapse upon cellular dissociation. J Immunol 174: 80–89. [PubMed: 15611230]
5. Wetzel SA, and Parker DC. 2006 MHC transfer from APC to T cells following antigen recognition. Crit Rev Immunol 26: 1–21. [PubMed: 16472066]
6. Shi M, Hao S, Chan T, and Xiang J. 2006 $CD4^+$ T cells stimulate memory $CD8^+$ T cell expansion via acquired pMHC I complexes and costimulatory molecules, and IL-2 secretion. J Leukoc Biol 80: 1354–1363. [PubMed: 16980510]
7. Hudrisier D, Aucher A, Puaux AL, Bordier C, and Joly E. 2007 Capture of target cell membrane components via trogocytosis is triggered by a selected set of surface molecules on T or B cells. J Immunol 178: 3637–3647. [PubMed: 17339461]
8. Adamopoulou E, Diekmann J, Tolosa E, Kuntz G, Einsele H, Rammensee HG, and Topp MS. 2007 Human $CD4^+$ T cells displaying viral epitopes elicit a functional virus-specific memory $CD8^+$ T cell response. J Immunol 178: 5465–5472. [PubMed: 17442927]
9. Umeshappa CS, Huang H, Xie Y, Wei Y, Mulligan SJ, Deng Y, and Xiang J. 2008 $CD4^+$ Th-APC with Acquired Peptide/MHC Class I and II Complexes Stimulate Type 1 Helper $CD4^+$ and Central Memory CD8+ T Cell Responses. The Journal of Immunology 182: 193–206.
10. Osborne DG, and Wetzel SA. 2012 Trogocytosis results in sustained intracellular signaling in $CD4^+$ T cells. J Immunol 189: 4728–4739. [PubMed: 23066151]
11. Riond J, Elhmouzi J, Hudrisier D, and Gairin JE. 2007 Capture of membrane components via trogocytosis occurs in vivo during both dendritic cells and target cells encounter by $CD8^+$ T cells. Scand J Immunol 66: 441–450. [PubMed: 17850589]
12. Gary R, Voelkl S, Palmisano R, Ullrich E, Bosch JJ, and Mackensen A. 2012 Antigen-Specific Transfer of Functional Programmed Death Ligand 1 from Human APCs onto $CD8^+$ T Cells via Trogocytosis. J Immunol 188: 744–752. [PubMed: 22174448]
13. Uzana R, Eisenberg G, Sagi Y, Frankenburg S, Merims S, Amariglio N, Yefenof E, Peretz T, Machlenkin A, and Lotem M. 2012 Trogocytosis Is a Gateway to Characterize Functional Diversity in Melanoma-Specific $CD8^+$ T Cell Clones. J Immunol 188: 632–640. [PubMed: 22156347]
14. Espinosa E, Tabiasco J, Hudrisier D, and Fournie JJ. 2002 Synaptic transfer by human gamma delta T cells stimulated with soluble or cellular antigens. J Immunol 168: 6336–6343. [PubMed: 12055250]
15. Zhou G, Ding ZC, Fu J, and Levitsky HI. 2011 Presentation of acquired peptide-MHC class II ligands by $CD4^+$ regulatory T cells or helper cells differentially regulates antigen-specific $CD4^+$ T cell response. J Immunol 186: 2148–2155. [PubMed: 21242518]

16. Aucher A, Magdeleine E, Joly E, and Hudrisier D. 2008 Capture of plasma membrane fragments from target cells by trogocytosis requires signaling in T cells but not in B cells. Blood 111: 5621–5628. [PubMed: 18381976]

17. Gardell JL, and Parker DC. 2017 CD40L is transferred to antigen-presenting B cells during delivery of T-cell help. Eur J Immunol 47: 41–50. [PubMed: 27753080]

18. Poupot M, Fournie JJ, and Poupot R. 2008 Trogocytosis and killing of IL-4-polarized monocytes by autologous NK cells. J Leukoc Biol 84: 1298–1305. [PubMed: 18687904]

19. Nakayama M, Takeda K, Kawano M, Takai T, Ishii N, and Ogasawara K. 2011 Natural killer (NK)-dendritic cell interactions generate MHC class II-dressed NK cells that regulate $CD4^+$ T cells. Proc Natl Acad Sci U S A 108: 18360–18365. [PubMed: 22042851]

20. Miner CA, Giri TK, Meyer CE, Shabsovich M, and Tripathy SK. 2015 Acquisition of activation receptor ligand by trogocytosis renders NK cells hyporesponsive. J Immunol 194: 1945–1953. [PubMed: 25582853]

21. Miyake K, Shiozawa N, Nagao T, Yoshikawa S, Yamanishi Y, and Karasuyama H. 2017 Trogocytosis of peptide-MHC class II complexes from dendritic cells confers antigen-presenting ability on basophils. Proc Natl Acad Sci U S A 114: 1111–1116. [PubMed: 28096423]

22. Daubeuf S, Lindorfer MA, Taylor RP, Joly E, and Hudrisier D. 2010 The direction of plasma membrane exchange between lymphocytes and accessory cells by trogocytosis is influenced by the nature of the accessory cell. J Immunol 184: 1897–1908. [PubMed: 20089699]

23. Sarvari AK, Doan-Xuan QM, Bacso Z, Csomos I, Balajthy Z, and Fesus L. 2015 Interaction of differentiated human adipocytes with macrophages leads to trogocytosis and selective IL-6 secretion. Cell Death Dis 6: e1613. [PubMed: 25611388]

24. Li KJ, Wu CH, Shen CY, Kuo YM, Yu CL, and Hsieh SC. 2016 Membrane Transfer from Mononuclear Cells to Polymorphonuclear Neutrophils Transduces Cell Survival and Activation Signals in the Recipient Cells via Anti-Extrinsic Apoptotic and MAP Kinase Signaling Pathways. PLoS One 11: e0156262. [PubMed: 27258015]

25. Valgardsdottir R, Cattaneo I, Klein C, Introna M, Figliuzzi M, and Golay J. 2017 Human neutrophils mediate trogocytosis rather than phagocytosis of CLL B cells opsonized with anti-CD20 antibodies. Blood 129: 2636–2644. [PubMed: 28288980]

26. Mercer F, Ng SH, Brown TM, Boatman G, and Johnson PJ. 2018 Neutrophils kill the parasite Trichomonas vaginalis using trogocytosis. PLoS Biol 16: e2003885. [PubMed: 29408891]

27. Zhang QJ, Li XL, Wang D, Huang XC, Mathis JM, Duan WM, Knight D, Shi R, Glass J, Zhang DQ, Eisenbach L, and Jefferies WA. 2008 Trogocytosis of MHC-I/peptide complexes derived from tumors and infected cells enhances dendritic cell cross-priming and promotes adaptive T cell responses. PLoS One 3: e3097. [PubMed: 18769733]

28. Bonaccorsi I, Morandi B, Antsiferova O, Costa G, Oliveri D, Conte R, Pezzino G, Vermiglio G, Anastasi GP, Navarra G, Munz C, Di Carlo E, Mingari MC, and Ferlazzo G. 2014 Membrane transfer from tumor cells overcomes deficient phagocytic ability of plasmacytoid dendritic cells for the acquisition and presentation of tumor antigens. J Immunol 192: 824–832. [PubMed: 24337377]

29. Haastert B, Mellanby RJ, Anderton SM, and O'Connor RA. 2013 T cells at the site of autoimmune inflammation show increased potential for trogocytosis. PLoS One 8: e81404. [PubMed: 24324692]

30. Tomaru U, Yamano Y, Nagai M, Maric D, Kaumaya PT, Biddison W, and Jacobson S. 2003 Detection of virus-specific T cells and $CD8^+$ T-cell epitopes by acquisition of peptide-HLA-GFP complexes: analysis of T-cell phenotype and function in chronic viral infections. Nat Med 9: 469–476. [PubMed: 12652294]

31. Rosenits K, Keppler SJ, Vucikuja S, and Aichele P. 2010 T cells acquire cell surface determinants of APC via in vivo trogocytosis during viral infections. Eur J Immunol 40: 3450–3457. [PubMed: 21080375]

32. Mukherjee S, Mukhopadhyay A, Andriani G, Machado FS, Ashton AW, Huang H, Weiss LM, and Tanowitz HB. 2015 *Trypanosoma cruzi* invasion is associated with trogocytosis. Microbes Infect 17: 62–70. [PubMed: 25448052]

33. Verwilghen J, Lovis R, De Boer M, Linsley PS, Haines GK, Koch AE, and Pope RM. 1994 Expression of functional B7 and CTLA4 on rheumatoid synovial T cells. J Immunol 153: 1378–1385. [PubMed: 7517975]
34. Brown R, Kabani K, Favaloro J, Yang S, Ho PJ, Gibson J, Fromm P, Suen H, Woodland N, Nassif N, Hart D, and Joshua D. 2012 CD86 or HLA-G can be transferred via trogocytosis from myeloma cells to T cells and are associated with poor prognosis. Blood 120: 2055–2063. [PubMed: 22705596]
35. Eisenberg G, Uzana R, Pato A, Frankenburg S, Merims S, Yefenof E, Ferrone S, Peretz T, Machlenkin A, and Lotem M. 2013 Imprinting of lymphocytes with melanoma antigens acquired by trogocytosis facilitates identification of tumor-reactive T cells. J Immunol 190: 5856–5865. [PubMed: 23626012]
36. LeMaoult J, Caumartin J, Daouya M, Favier B, Le Rond S, Gonzalez A, and Carosella ED. 2007 Immune regulation by pretenders: cell-to-cell transfers of HLA-G make effector T cells act as regulatory cells. Blood 109: 2040–2048. [PubMed: 17077329]
37. Ahmed KA, and Xiang J. 2011 Mechanisms of cellular communication through intercellular protein transfer. J Cell Mol Med 15: 1458–1473. [PubMed: 20070437]
38. Brown R, Suen H, Favaloro J, Yang S, Ho PJ, Gibson J, and Joshua D. 2012 Trogocytosis generates acquired regulatory T cells adding further complexity to the dysfunctional immune response in multiple myeloma. Oncoimmunology 1: 1658–1660. [PubMed: 23264928]
39. Gu P, Gao JF, D'Souza CA, Kowalczyk A, Chou KY, and Zhang L. 2012 Trogocytosis of CD80 and CD86 by induced regulatory T cells. Cell Mol Immunol 9: 136–146. [PubMed: 22307040]
40. Shao Z, Harfuddin Z, Pang WL, Nickles E, Koh LK, and Schwarz H. 2015 Trogocytic CD137 transfer causes an internalization of CD137 ligand on murine APCs leading to reduced T cell costimulation. J Leukoc Biol 97: 909–919. [PubMed: 25765680]
41. Barinov A, Galgano A, Krenn G, Tanchot C, Vasseur F, and Rocha B. 2017 CD4/CD8/Dendritic cell complexes in the spleen: $CD8^+$ T cells can directly bind CD4+ T cells and modulate their response. PLoS One 12: e0180644. [PubMed: 28686740]
42. Hudrisier D, Riond J, Garidou L, Duthoit C, and Joly E. 2005 T cell activation correlates with an increased proportion of antigen among the materials acquired from target cells. Eur J Immunol 35: 2284–2294. [PubMed: 16021601]
43. Huang JF, Yang Y, Sepulveda H, Shi W, Hwang I, Peterson PA, Jackson MR, Sprent J, and Cai Z. 1999 TCR-Mediated internalization of peptide-MHC complexes acquired by T cells. Science 286: 952–954. [PubMed: 10542149]
44. Hwang I, Huang JF, Kishimoto H, Brunmark A, Peterson PA, Jackson MR, Surh CD, Cai Z, and Sprent J. 2000 T cells can use either T cell receptor or CD28 receptors to absorb and internalize cell surface molecules derived from antigen-presenting cells. J Exp Med 191: 1137–1148. [PubMed: 10748232]
45. Rechavi O, Goldstein I, Vernitsky H, Rotblat B, and Kloog Y. 2007 Intercellular transfer of oncogenic H-Ras at the immunological synapse. PLoS One 2: e1204. [PubMed: 18030338]
46. Monks CR, Freiberg BA, Kupfer H, Sciaky N, and Kupfer A. 1998 Three-dimensional segregation of supramolecular activation clusters in T cells. Nature 395: 82–86. [PubMed: 9738502]
47. Qi SY, Groves JT, and Chakraborty AK. 2001 Synaptic pattern formation during cellular recognition. Proc Natl Acad Sci U S A 98: 6548–6553. [PubMed: 11371622]
48. Grakoui A, Bromley SK, Sumen C, Davis MM, Shaw AS, Allen PM, and Dustin ML. 1999 The immunological synapse: a molecular machine controlling T cell activation. Science 285: 221–227. [PubMed: 10398592]
49. van der Merwe PA, Davis SJ, Shaw AS, and Dustin ML. 2000 Cytoskeletal polarization and redistribution of cell-surface molecules during T cell antigen recognition. Semin Immunol 12: 5–21. [PubMed: 10723794]
50. Liu H, Rhodes M, Wiest DL, and Vignali DA. 2000 On the dynamics of TCR:CD3 complex cell surface expression and downmodulation. Immunity 13: 665–675. [PubMed: 11114379]
51. Martinez-Martin N, Fernandez-Arenas E, Cemerski S, Delgado P, Turner M, Heuser J, Irvine DJ, Huang B, Bustelo XR, Shaw A, and Alarcon B. 2011 T cell receptor internalization from the

immunological synapse is mediated by TC21 and RhoG GTPase-dependent phagocytosis. Immunity 35: 208–222. [PubMed: 21820331]

52. Dopfer EP, Minguet S, and Schamel WW. 2011 A new vampire saga: the molecular mechanism of T cell trogocytosis. Immunity 35: 151–153. [PubMed: 21867922]
53. Xiang J, Huang H, and Liu Y. 2005 A new dynamic model of $CD8^+$ T effector cell responses via $CD4^+$ T helper-antigen-presenting cells. J Immunol 174: 7497–7505. [PubMed: 15944248]
54. Amiot L, Vu N, and Samson M. 2015 Biology of the immunomodulatory molecule HLA-G in human liver diseases. J Hepatol 62: 1430–1437. [PubMed: 25772038]
55. Nolte-'t Hoen EN, Wagenaar-Hilbers JP, Peters PJ, Gadella BM, van Eden W, and Wauben MH. 2004 Uptake of membrane molecules from T cells endows antigen-presenting cells with novel functional properties. Eur J Immunol 34: 3115–3125. [PubMed: 15459903]
56. Nakayama M 2014 Antigen Presentation by MHC-Dressed Cells. Front Immunol 5: 672. [PubMed: 25601867]
57. Romagnoli PA, Premenko-Lanier MF, Loria GD, and Altman JD. 2013 CD8 T cell memory recall is enhanced by novel direct interactions with CD4 T cells enabled by MHC class II transferred from APCs. PLoS One 8: e56999. [PubMed: 23441229]
58. Romagnoli P, Hudrisier D, and van Meerwijk JP. 2005 Molecular Signature of Recent Thymic Selection Events on Effector and Regulatory $CD4^+$ T Lymphocytes. J Immunol 175: 5751–5758. [PubMed: 16237066]
59. Game DS, Rogers NJ, and Lechler RI. 2005 Acquisition of HLA-DR and costimulatory molecules by T cells from allogeneic antigen presenting cells. Am J Transplant 5: 1614–1625. [PubMed: 15943619]
60. Helft J, Jacquet A, Joncker NT, Grandjean I, Dorothee G, Kissenpfennig A, Malissen B, Matzinger P, and Lantz O. 2008 Antigen-specific T-T interactions regulate CD4 T-cell expansion. Blood 112: 1249–1258. [PubMed: 18539897]
61. Bahcheli D, Hay V, Nadeau JL, and Piccirillo CA. 2011 Transfer of cell membrane components via trogocytosis occurs in CD4+ $Foxp3^+$ $CD25^+$ regulatory T-cell contact-dependent suppression. Autoimmunity 44: 607–615. [PubMed: 21604971]
62. Hsu P, Santner-Nanan B, Joung S, Peek MJ, and Nanan R. 2014 Expansion of $CD4^+$ HLA-G^+ T Cell in human pregnancy is impaired in pre-eclampsia. Am J Reprod Immunol 71: 217–228. [PubMed: 24383466]
63. Gonzalez A, Rebmann V, LeMaoult J, Horn PA, Carosella ED, and Alegre E. 2012 The immunosuppressive molecule HLA-G and its clinical implications. Crit Rev Clin Lab Sci 49: 63–84. [PubMed: 22537084]
64. Zhou J, Tagaya Y, Tolouei-Semnani R, Schlom J, and Sabzevari H. 2005 Physiological relevance of antigen presentasome (APS), an acquired MHC/costimulatory complex, in the sustained activation of CD4+ T cells in the absence of APCs. Blood 105: 3238–3246. [PubMed: 15637136]
65. Seder RA, Paul WE, Davis MM, and Fazekas de St Groth B. 1992 The presence of interleukin 4 during in vitro priming determines the lymphokine-producing potential of CD4+ T cells from T cell receptor transgenic mice. J Exp Med 176: 1091–1098. [PubMed: 1328464]
66. Thauland TJ, Koguchi Y, Wetzel SA, Dustin ML, and Parker DC. 2008 Th1 and Th2 cells form morphologically distinct immunological synapses. J Immunol 181: 393–399. [PubMed: 18566405]
67. Faroudi M, Zaru R, Paulet P, Muller S, and Valitutti S. 2003 Cutting edge: T lymphocyte activation by repeated immunological synapse formation and intermittent signaling. J Immunol 171: 1128–1132. [PubMed: 12874197]
68. Simms PE, and Ellis TM. 1996 Utility of flow cytometric detection of CD69 expression as a rapid method for determining poly- and oligoclonal lymphocyte activation. Clin Diagn Lab Immunol 3: 301–304. [PubMed: 8705673]
69. Chan AC, Irving BA, Fraser JD, and Weiss A. 1991 The zeta chain is associated with a tyrosine kinase and upon T-cell antigen receptor stimulation associates with ZAP-70, a 70-kDa tyrosine phosphoprotein. Proc Natl Acad Sci U S A 88: 9166–9170. [PubMed: 1717999]
70. Straus DB, and Weiss A. 1993 The CD3 chains of the T cell antigen receptor associate with the ZAP-70 tyrosine kinase and are tyrosine phosphorylated after receptor stimulation. J Exp Med 178: 1523–1530. [PubMed: 7693848]

71. Kupfer A, Mosmann TR, and Kupfer H. 1991 Polarized expression of cytokines in cell conjugates of helper T cells and splenic B cells. Proc Natl Acad Sci U S A 88: 775–779. [PubMed: 1825141]
72. Fairfax KC, Everts B, Amiel E, Smith AM, Schramm G, Haas H, Randolph GJ, Taylor JJ, and Pearce EJ. 2015 IL-4-secreting secondary T follicular helper (Tfh) cells arise from memory T cells, not persisting Tfh cells, through a B cell-dependent mechanism. J Immunol 194: 2999–3010. [PubMed: 25712216]
73. Schmidt-Weber CB, Rao A, and Lichtman AH. 2000 Integration of TCR and IL-4 signals through STAT6 and the regulation of IL-4 gene expression. Mol Immunol 37: 767–774. [PubMed: 11275261]
74. Cook KD, and Miller J. 2010 TCR-dependent translational control of GATA-3 enhances Th2 differentiation. J Immunol 185: 3209–3216. [PubMed: 20696860]
75. Zhu J, and Paul WE. 2010 $CD4^+$ T cell plasticity-Th2 cells join the crowd. Immunity 32: 11–13. [PubMed: 20152167]
76. Krawczyk CM, Shen H, and Pearce EJ. 2007 Functional plasticity in memory T helper cell responses. J Immunol 178: 4080–4088. [PubMed: 17371962]
77. Magombedze G, Reddy PB, Eda S, and Ganusov VV. 2013 Cellular and population plasticity of helper $CD4^+$ T cell responses. Front Physiol 4: 206. [PubMed: 23966946]
78. Szabo SJ, Jacobson NG, Dighe AS, Gubler U, and Murphy KM. 1995 Developmental commitment to the Th2 lineage by extinction of IL-12 signaling. Immunity 2: 665–675. [PubMed: 7796298]
79. Panzer M, Sitte S, Wirth S, Drexler I, Sparwasser T, and Voehringer D. 2012 Rapid in vivo conversion of effector T cells into Th2 cells during helminth infection. J Immunol 188: 615–623. [PubMed: 22156341]
80. Howard JG, Hale C, and Chan-Liew WL. 1980 Immunological regulation of experimental cutaneous leishmaniasis. 1. Immunogenetic aspects of susceptibility to Leishmania tropica in mice. Parasite Immunol 2: 303–314. [PubMed: 7220075]
81. Conboy IM, DeKruyff RH, Tate KM, Cao ZA, Moore TA, Umetsu DT, and Jones PP. 1997 Novel genetic regulation of T helper 1 (Th1)/Th2 cytokine production and encephalitogenicity in inbred mouse strains. J Exp Med 185: 439–451. [PubMed: 9053444]
82. Zhu J, Yamane H, and Paul WE. 2010 Differentiation of effector CD4 T cell populations (*). Annu Rev Immunol 28: 445–489. [PubMed: 20192806]
83. Tubo NJ, and Jenkins MK. 2014 TCR signal quantity and quality in $CD4^+$ T cell differentiation. Trends Immunol 35: 591–596. [PubMed: 25457838]
84. van Panhuys N, Klauschen F, and Germain RN. 2014 T-cell-receptor-dependent signal intensity dominantly controls CD4(+) T cell polarization In Vivo. Immunity 41: 63–74. [PubMed: 24981853]
85. Keck S, Schmaler M, Ganter S, Wyss L, Oberle S, Huseby ES, Zehn D, and King CG. 2014 Antigen affinity and antigen dose exert distinct influences on CD4 T-cell differentiation. Proc Natl Acad Sci U S A 111: 14852–14857. [PubMed: 25267612]
86. Tao X, Constant S, Jorritsma P, and Bottomly K. 1997 Strength of TCR signal determines the costimulatory requirements for Th1 and Th2 $CD4^+$ T cell differentiation. J Immunol 159: 5956–5963. [PubMed: 9550393]
87. Brogdon JL, Leitenberg D, and Bottomly K. 2002 The potency of TCR signaling differentially regulates NFATc/p activity and early IL-4 transcription in naive $CD4^+$ T cells. J Immunol 168: 3825–3832. [PubMed: 11937535]
88. Constant S, Pfeiffer C, Woodard A, Pasqualini T, and Bottomly K. 1995 Extent of T cell receptor ligation can determine the functional differentiation of naive $CD4^+$ T cells. J Exp Med 182: 1591–1596. [PubMed: 7595230]
89. Turner MS, Isse K, Fischer DK, Turnquist HR, and Morel PA. 2014 Low TCR signal strength induces combined expansion of Th2 and regulatory T cell populations that protect mice from the development of type 1 diabetes. Diabetologia 57: 1428–1436. [PubMed: 24737163]
90. van Panhuys N 2016 TCR Signal Strength Alters T-DC Activation and Interaction Times and Directs the Outcome of Differentiation. Front Immunol 7: 6. [PubMed: 26834747]

91. Leitenberg D, Boutin Y, Constant S, and Bottomly K. 1998 CD4 regulation of TCR signaling and T cell differentiation following stimulation with peptides of different affinities for the TCR. J Immunol 161: 1194–1203. [PubMed: 9686579]

92. Leitenberg D, and Bottomly K. 1999 Regulation of naive T cell differentiation by varying the potency of TCR signal transduction. Semin Immunol 11: 283–292. [PubMed: 10441214]

93. Wetzel SA, McKeithan TW, and Parker DC. 2002 Live-cell dynamics and the role of costimulation in immunological synapse formation. J Immunol 169: 6092–6101. [PubMed: 12444111]

94. Vella AT, Dow S, Potter TA, Kappler J, and Marrack P. 1998 Cytokine-induced survival of activated T cells in vitro and in vivo. Proc Natl Acad Sci U S A 95: 3810–3815. [PubMed: 9520449]

95. Ebihara M, Hattori M, and Yoshida T. 2007 Distinctly different sensitivity in the induction and reversal of anergy of Th1 and Th2 cells. Biosci Biotechnol Biochem 71: 130–137. [PubMed: 17213641]

96. Morris SC, Gause WC, and Finkelman FD. 2000 IL-4 suppression of in vivo T cell activation and antibody production. J Immunol 164: 1734–1740. [PubMed: 10657618]

97. Linterman MA, and Vinuesa CG. 2010 Signals that influence T follicular helper cell differentiation and function. Semin Immunopathol 32: 183–196. [PubMed: 20107805]

98. Glatman Zaretsky A, Taylor JJ, King IL, Marshall FA, Mohrs M, and Pearce EJ. 2009 T follicular helper cells differentiate from Th2 cells in response to helminth antigens. J Exp Med 206: 991–999. [PubMed: 19380637]

Key Points

1. 1. Trogocytosis-mediated signaling promotes IL-4 expression and T_H2 differentiation.
2. 2. T_H2 cells perform trogocytosis more efficiently than T_H1 or non-polarized cells.
3. 3. *In vivo* generated, trogocytosis-positive cells are predominantly T_H2.

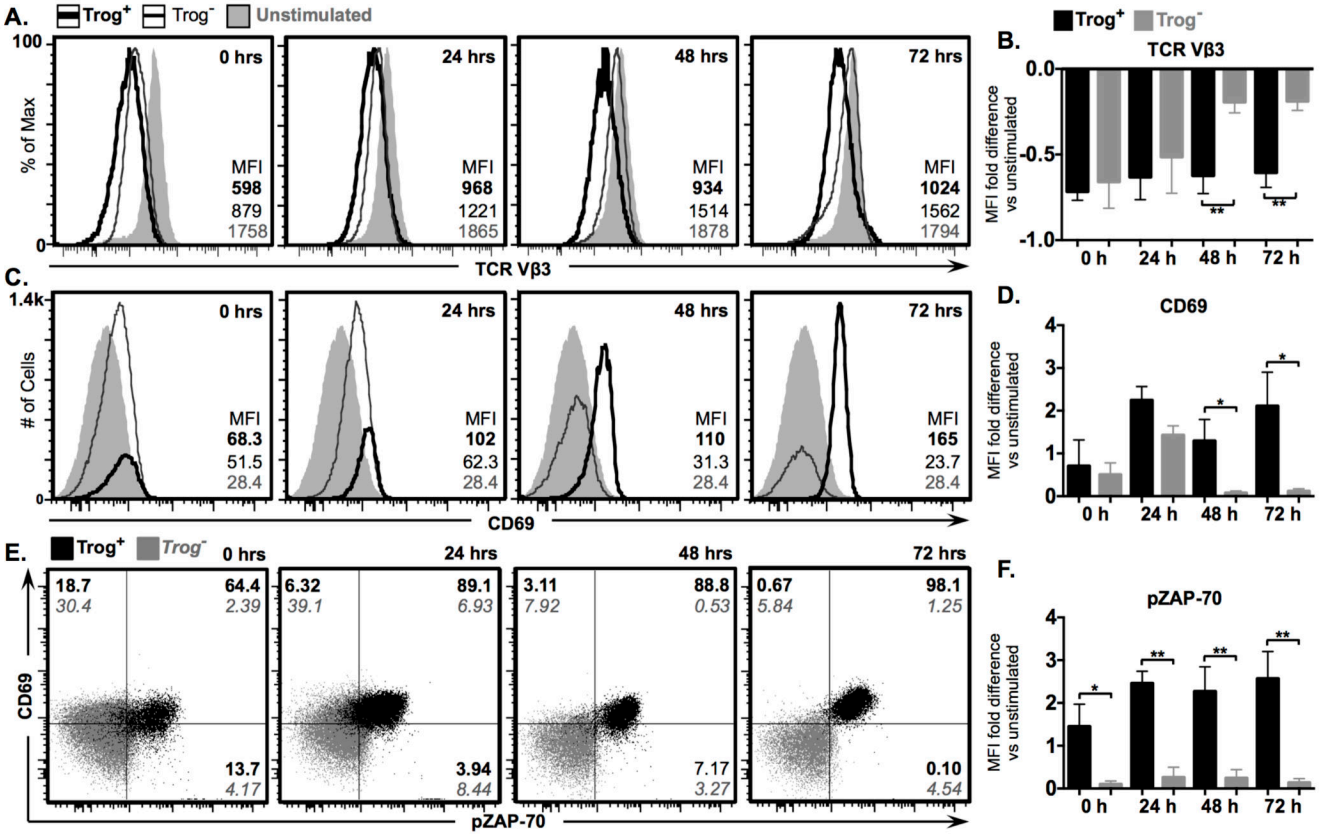

Figure 1. Sustained TCR signaling, survival, and activation in trog$^+$, but not trog$^-$, CD4$^+$ T cells after APC removal.

CD4$^+$ T cells recovered from standard *in vitro* trogocytosis assay were cultured at low density (10^4 cells/ml) for 72 hours. At indicated time-points, expression of TCR Vβ3, CD69 and phosphorylated ZAP-70 were determined via flow cytometry. **(A)** Representative histograms showing TCR Vβ3 expression in trog$^+$ *(thick black line)*, trog$^-$ *(thin black line)*, and unstimulated *(shaded grey)* cells. **(B)** Mean fold-difference in TCR Vβ3 expression between trog$^+$ *(black)* and trog$^-$ *(grey)* cells compared to unstimulated T cell blasts. **(C)** CD69 expression in in trog$^+$ *(thick black line)*, trog$^-$ *(thin black line)*, and unstimulated *(shaded grey)* cells. Numbers represent geometric mean fluorescence intensity (MFI) of respective populations. **(D)** Mean fold-difference in CD69 expression between trog$^+$ *(black)* and trog$^-$ *(grey*) cells compared to unstimulated T cell blasts. **(E)** 2D plots showing phosphorylated ZAP-70 vs CD69 in trog$^+$ *(black)* and trog$^-$ *(grey)* CD4$^+$ T cells. Quadrant gates were determined by unstimulated CD4$^+$ cells, where >99% of cells were contained in the bottom left quadrant. **(F)** Mean fold-difference in the MFI of phosphorylated ZAP-70 in trog$^+$ *(black)* and trog$^-$ *(grey)* cells compared to unstimulated CD4$^+$ cells. In Figs. B, D, and F, error bars represent ±SEM from three independent experiments with * = p≤ 0.05 and ** = p≤ 0.01. Unstimulated samples represent CD4$^+$ T cell blasts prior to the trogocytosis assay. All data is representative of thee independent experiments.

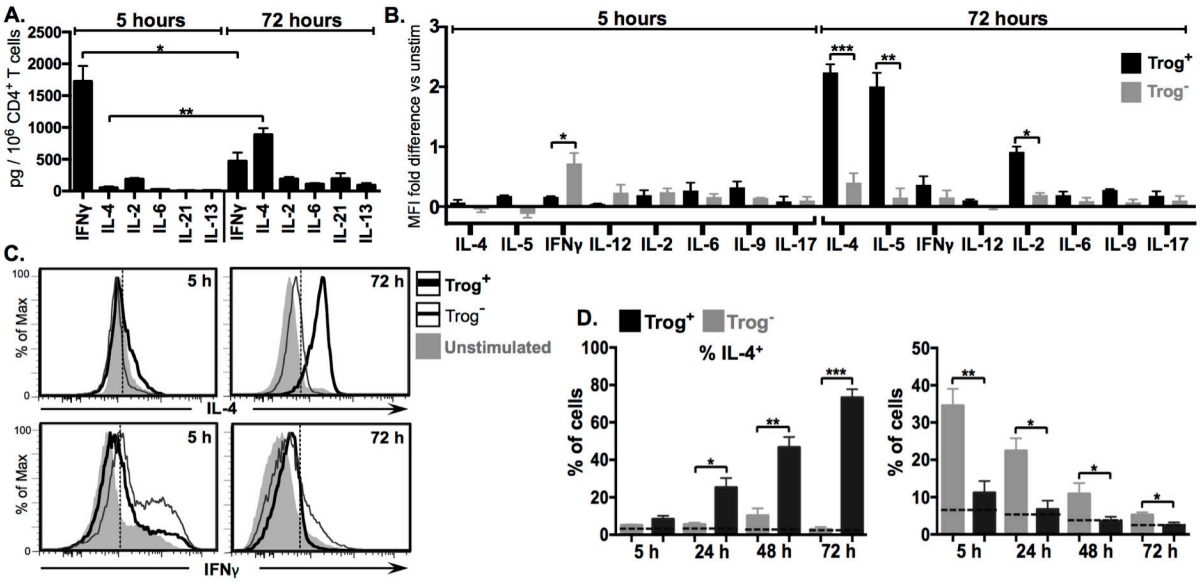

Figure 2. After APC removal, trog$^+$ cells increase expression of T_H2-associated effector cytokines, while trog$^-$ cells express decreasing levels of T_H1-associated cytokines.

Expression of cytokines in CD4$^+$ T cells recovered from a standard *in vitro* trogocytosis assay was assessed at indicated time points by flow cytometry. **(A)** Mean levels of subset-characteristic T-helper cytokines in culture supernatant of total recovered T cells at 5 hours *(grey)* and 72 hours *(black)* post trogocytosis-assay. **(B)** Mean fold-difference in the expression of subset characteristic T-helper cytokines between trog$^+$ *(black)* and trog$^-$ *(grey)* cells, compared to unstimulated CD4$^+$ T cells, at 5 and 72 hours post-recovery, as measured by intracellular cytokine staining (ICS) MFI. **(C)** Representative histogram plots of ICS data showing fluorescence intensity of IL-4 *(top)* and IFNγ *(bottom)* in trog$^+$ *(thick black line)* and trog$^-$ *(thin black line)* CD4$^+$ T cells. Unstimulated controls are shown in shaded grey for comparison. Dashed vertical line represents the maximum MFI for >99% relevant isotype control. **(D)** Frequency of IL-4$^+$ *(left)* or IFNγ^+ *(right)* CD4$^+$, trog$^+$ *(black)*, and trog$^-$ cells over 72 hours after APC removal. Dashed horizontal line represents mean percentage of unstimulated CD4$^+$ T cells for respective cytokines. In Figs. A, C and F, error bars represent ±SEM from three independent experiments, where * = p≤ 0.05, ** = p≤ 0.01, and *** = p≤ 0.001. In Figs B and D, dotted vertical lines represent the fluorescence intensity >99% of recovered CD4$^+$ cells stained with respective isotype controls. All ICS data is representative of at least three independent experiments.

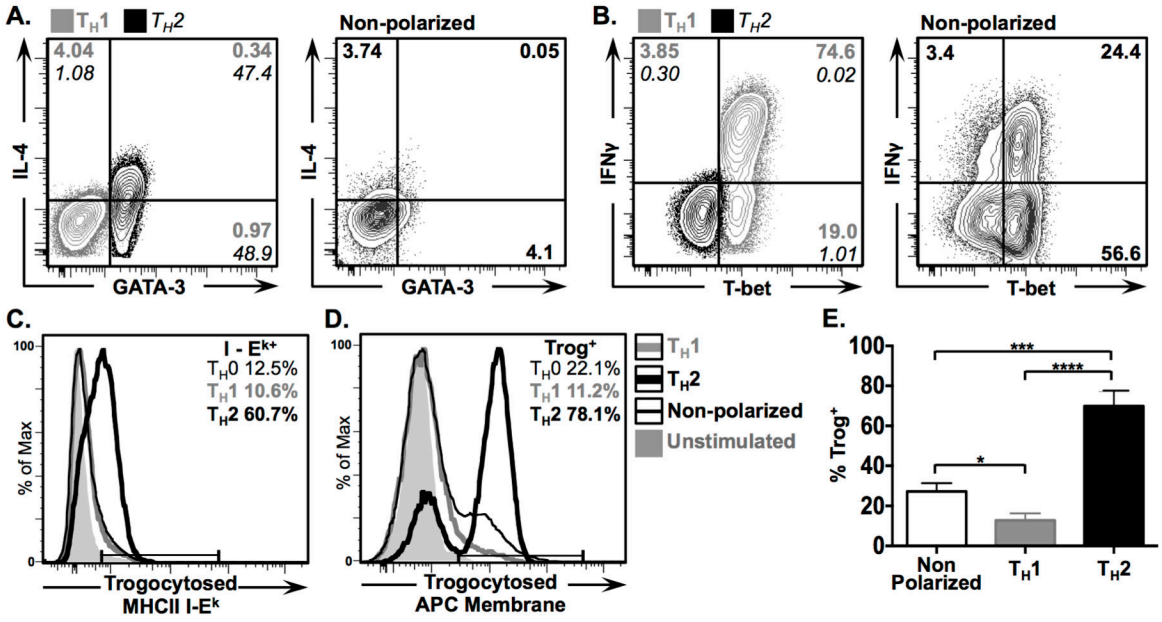

Figure 3. In vitro polarized T_H2 $CD4^+$ T cells are more efficient at performing trogocytosis than T_H1 and non-polarized cells.

Non-polarized and *in vitro* polarized T_H1 and T_H2 T cell blasts were used in standard *in vitro* trogocytosis assay and expression of IL-4, GATA-3, IFNγ and T-bet in recovered T cells was assessed via flow cytometry. **(A & B)** 2D plots showing fluorescence intensity of (A) IL-4 vs. GATA-3, and (B) IFNγ vs. T-bet in polarized T_H2 *(grey)* and T_H1 *(black)*, and non-polarized cells, 1 hour post recovery. Numbers in corners represent frequencies of cells in respective quadrants. **(C & D)** Histogram overlays showing the frequency of trogocytosed *(C)* MHCII I-E^k and *(D)* biotinylated APC membrane by polarized T_H1 *(grey line)* T_H2 *(thick black line)*, and non-polarized cells *(thin black line)*, with unstimulated controls in shaded grey for comparison. **(E)** Mean frequency of $trog^+$ cells from non-polarized *(left)*, T_H1 *(middle)*, and T_H2 *(right)* $CD4^+$ cells 1 hour post-recovery. Error bars represent ±SEM from three independent experiments, * = p≤ 0.05, *** = p≤ 0.001, and **** = p≤ 0.0001. All data shown is representative of three independent experiments.

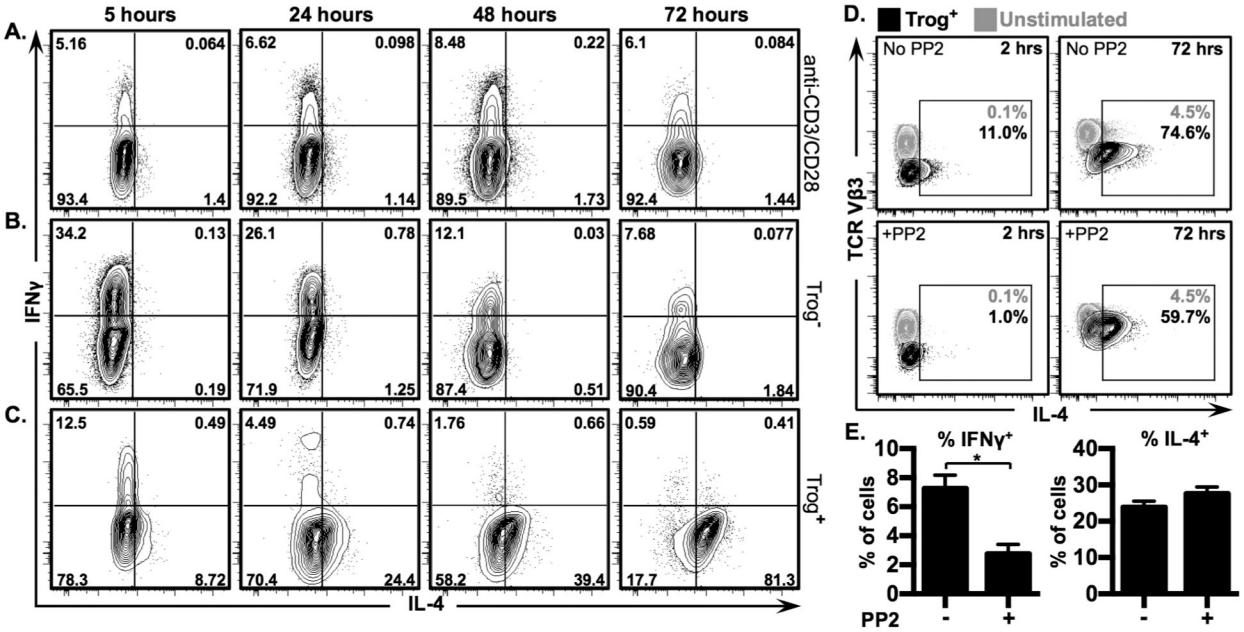

Figure 4. Trogocytosis-mediated signaling drives IL-4, but not IFNγ, expression in trog$^+$ cells.

Non-polarized CD4$^+$ T cells were used in a standard *in* vitro trogocytosis assay, or were stimulated with plate-bound anti-CD3 + anti-CD28. Levels of IL-4 and IFN γ were measured by ICS and analyzed via flow cytometry. Representative 2D flow plots show fluorescence intensity of IL-4 vs IFNγ in **(A)** Ab-stimulated blasts, **(B)** trog$^-$ cells, and **(C)** trog$^+$ cells, at indicted time points post-recovery. Gates were established using respective isotype-control staining where >99% of CD4$^+$ cells stained with isotype controls fell in the lower left quadrant. Numbers in corners represent frequency of cells in respective quadrants. Data are representative of at least 3 independent experiments. **(D)** Immediately after recovery from an *in vitro* trogocytosis assay, cells were left untreated *(top row)* or were treated for 20 minutes with 20 μM PP2 *(bottom row)* to halt TCR signaling. PP2 was removed from cultures and cells were analyzed at 2 *(left column)*, and 72 hours *(right column)*, after PP2 removal. Trog$^+$ cells are shown in black, compared to unstimulated cells in grey. Numbers represent frequency of cells included in respective gates. **(E)** Mean frequency of IFNγ$^+$ and IL-4$^+$ trog$^+$ cells, 24 hours after PP2 removal, compared to untreated trog$^+$ cells. Error bars represent ±SEM from three independent experiments, * = p≤ 0.05. All data is representative of at least three independent experiments.

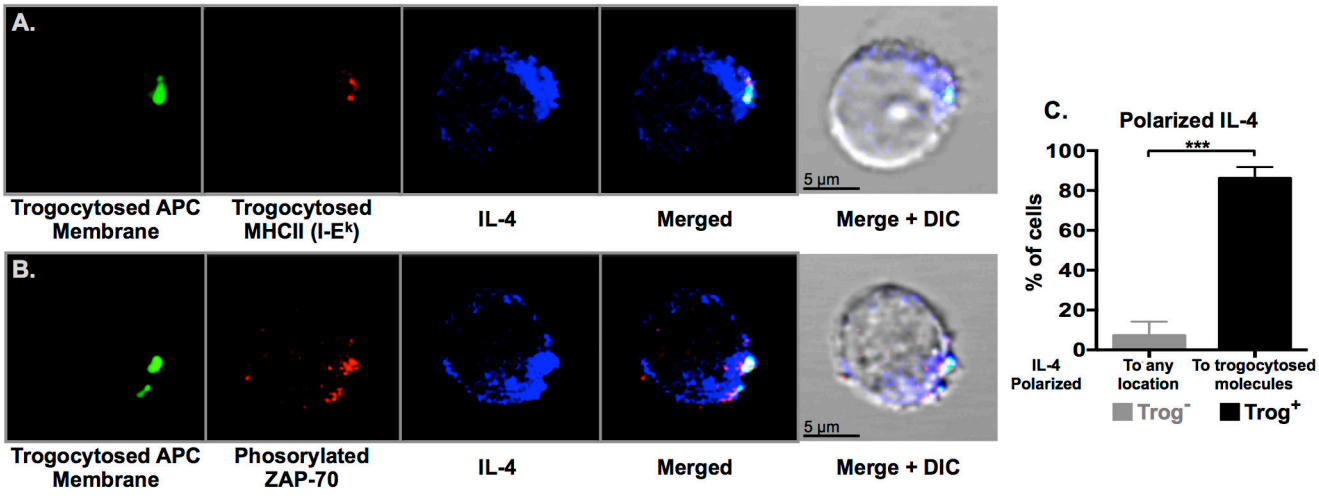

Figure 5. IL-4 is polarized towards trogocytosed molecules and the location of active TCR signaling.

$CD4^+$ T cells were analyzed by confocal microscopy 72-hours after recovery from a standard *in vitro* trogocytosis assay. Representative optical sections of $trog^+$ cells are shown with **(A)** trogocytosed APC membrane proteins *(green)*, trogocytosed I-E^k (*red)*, and intracellular IL-4 *(blue)*. **(B)** Trogocytosed APC membrane proteins *(green)*, phosphorylated-Zap-70 (*red)* and intracellular IL-4 *(blue)*. Data is representative of five independent experiments, with over 120 individual $trog^+$ $CD4^+$ cells analyzed in total. **(C)** IL-4^+ $trog^-$ *(grey)* and $trog^+$ *(black)* cells were analyzed for IL-4 polarization, as defined by the localization of intracellular IL-4 to any constrained area for the $trog^-$ cells, and polarization towards trogocytosed molecules in the $trog^+$ cells. Error bars represent ±SEM from three independent experiments, *** = $p \leq 0.001$.

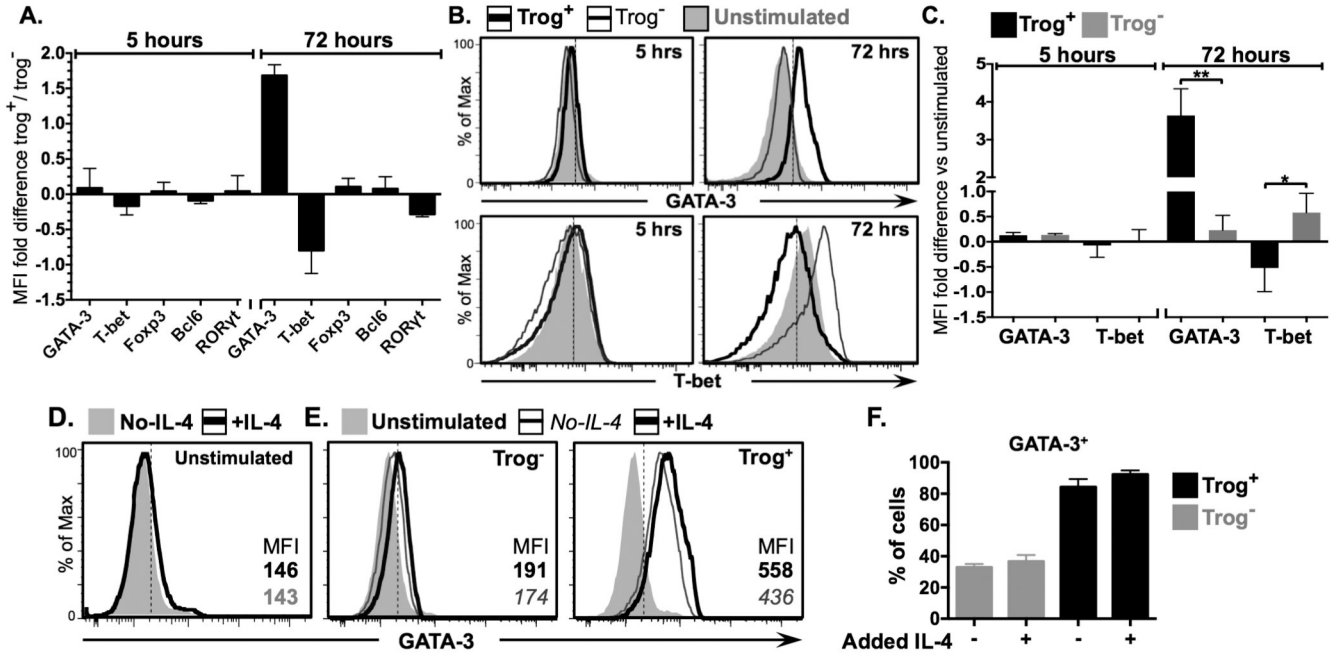

Figure 6. Trogocytosis-mediated signaling drives GATA-3 expression in trog$^+$ cells.

CD4$^+$ T cells were recovered from a standard *in vitro* trogocytosis assay and characteristic T-helper subset transcription factor expression was examined by flow cytometry. **(A)** Mean fold-difference in expression of indicated transcription factors between trog$^+$ cells and trog$^-$ cells at five, and 72, hours post-recovery as determined by MFI. **(B)** Representative histograms of samples in 6A showing GATA-3 *(top)* and T-bet *(bottom)* levels in trog$^+$ *(thick black line)* and trog$^-$ *(thin black line)* cells, with unstimulated control cells shown in shaded grey for comparison. **(C)** Mean fold-difference in GATA-3 and T-bet expression between trog$^+$ *(black)* and trog$^-$ *(grey)* cells compared to unstimulated cells, at 5, and 72 hours post recovery. **(D-E)** Exogenous IL-4 (20 μg/ml) was added to recovered cell cultures immediately after the trogocytosis assay, and supplemented 24 hours later. (D) GATA-3 levels 72 hours post-recovery are shown for (left) unstimulated cells with (*black line*) and without *(shaded grey)* supplemental IL-4 (E) GATA-3 levels 72 hours post-recovery trog$^-$ cells *(left)*, and trog$^+$ cells *(right)*, with *(black line)* or without *(thin grey line)* supplemental IL-4. Unstimulated cells cultured without supplemented IL-4 in shaded grey are included for comparison. (F). Mean frequency of GATA-3$^+$ trog$^-$ *(grey)* and trog$^+$ *(black)* cells from cultures with, and without, supplemented IL-4. In Figs. A, C, and F, error bars represent ±SEM from three independent experiments, * = p≤ 0.05, ** = p≤ 0.01. In Figs. B and D, dotted vertical lines represent the fluorescence intensity >99% of recovered CD4$^+$ cells stained with respective isotype controls. All data is representative of three independent experiments.

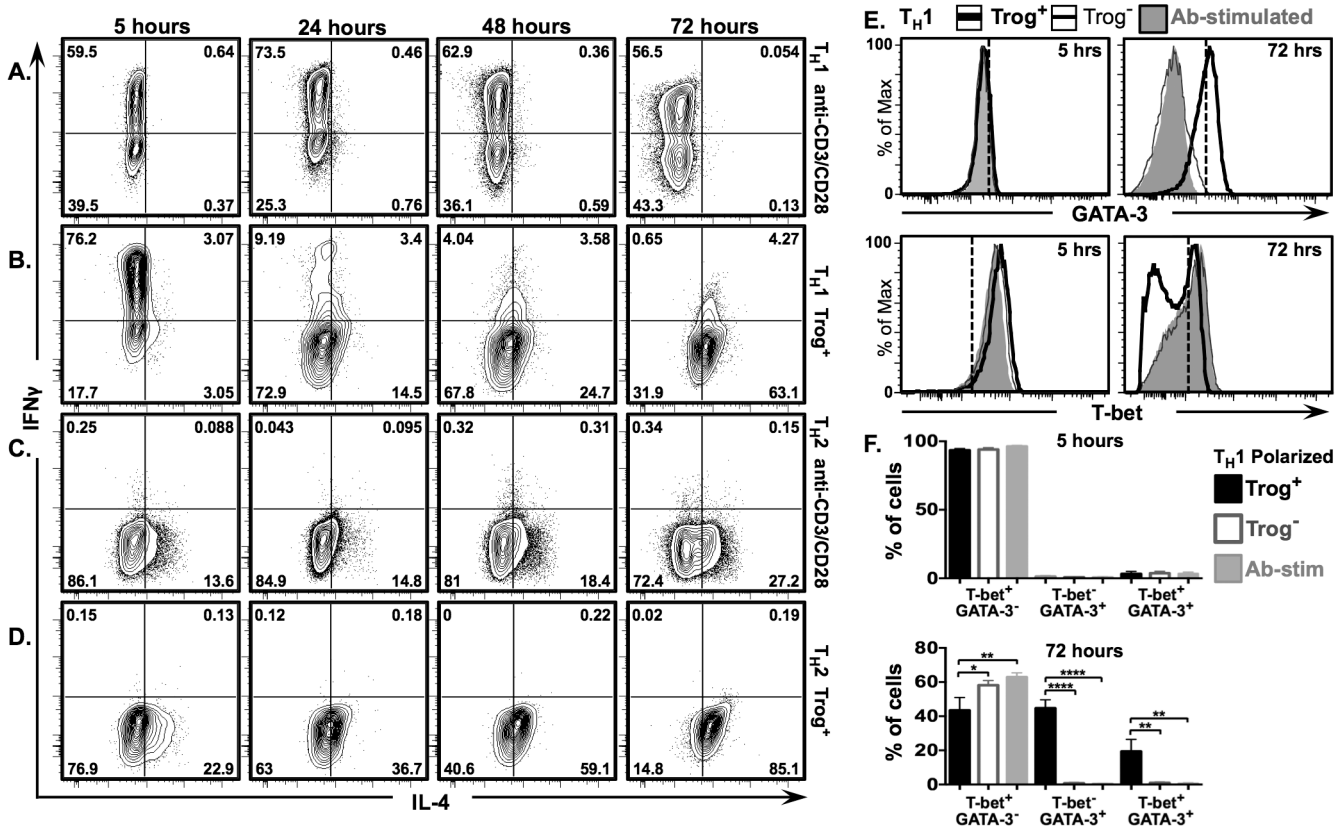

Figure 7. ***IL-4 expression increases and* IFNγ *expression decreases in polarized T_H1 trog$^+$ cells after removal of APC.***

In vitro polarized T_H1 and T_H2 CD4$^+$ T cells were used in a standard *in vitro* trogocytosis assay. In parallel, aliquots of polarized cells were stimulated with plate-bound anti-CD3 + anti-CD28 Abs. Fluorescence intensity of IL-4 vs. IFNγ is displayed in representative 2D scatter plots at 5 hrs. *(left)*, 24 hrs., *(2nd from left)*, 48 hrs. *(2nd from right)*, and 72 hrs. *(right)*for **(A)** anti-CD3 + anti-CD28 stimulated T_H1 polarized cells, **(B)** T_H1 polarized trog$^+$ cells **(C)** anti-CD3 + anti-CD28 stimulated T_H2 polarized, and **(D)** T_H2 polarized trog$^+$ cells. Numbers represent frequency of cells in each quadrant. **(E)** Representative histograms showing intensity of GATA-3 *(top)* and T-bet *(bottom)* expression in T_H1 polarized trog$^+$ *(thick black line)* and trog$^-$ *(thin black line)* cells, compared to anti-CD3/CD28 stimulated blasts *(shaded grey)*, at 5 *(left)*, and 72 *(right)*, hours post-recovery. **(F)** Mean frequency of T-bet$^+$ GATA-3$^-$ *(left)*, T-bet$^-$ GATA-3$^+$ *(middle)*, and T-bet$^+$ GATA-3$^+$ *(right)*, *in vitro* polarized T_H1 trog$^+$ *(black)*, trog$^-$ *(grey outline)*, and anti-CD3/CD28 stimulated cells *(shaded grey)* at 5 *(top)*, and 72 *(bottom)* hours post-recovery. Error bars represent ±SEM from three independent experiments, * = p≤ 0.05, ** = p≤ 0.01, *** = p≤ 0.001, and **** = p≤ 0.0001. All data is representative of three independent experiments.

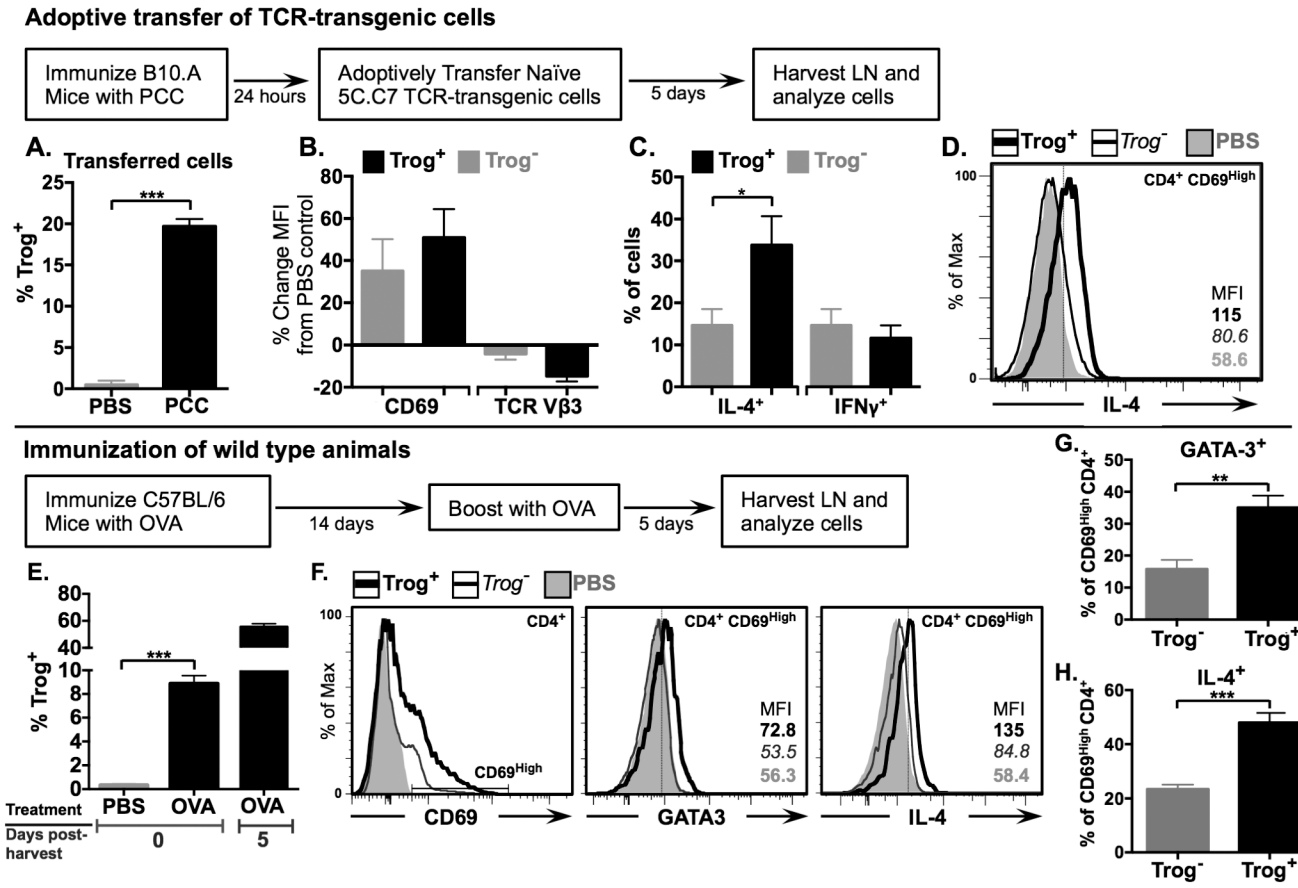

Figure 8. In vivo, trog^{+} CD4^{+} T cells display a T$_{H}$2 phenotype

(A-D) Adoptive transfer. B10.A mice (n=3) were immunized s.c. with 300 μg of PCC protein, or PBS as a control. Twenty-four hours after immunization, 2 × 10^{6} naïve CFSE-labeled 5C.C7 T cells were adoptively transferred into immunized B10.A recipients. Cells were harvested and analyzed via flow cytometry 5 days following adoptive transfer. **(A)** Mean frequency of trog^{+} cells from recovered adoptively transferred cells in PBS injected *(grey)* and PCC immunized *(black)*, mice. **(B)** Mean percent change in CD69 *(left)* and TCR Vβ3 *(right)* expression in trog^{+} *(black)* and trog^{-} *(grey)* recovered, adoptively transferred CD4^{+} cells, compared to recovered, adoptively transferred CD4^{+} cells, from PBS control animals as determined by in MFI. **(B)** Frequency of IL-4^{+} *(left)* and IFNγ $^{+}$ *(right)* trog^{+} *(black)* and trog^{-} *(grey)* CD4^{+} CD69^{High} adoptively transferred cells recovered from PCC immunized animals **(D)** Representative histogram of intracellular IL-4 expression of trog^{+} *(thick black line)* and trog^{-} *(thin black line)* CD4^{+} CD69^{High} adoptively transferred cells recovered from PCC immunized animals, compared to adoptively transferred CD4^{+} T cells recovered from PBS control animals *(shaded grey)*. In Figs. A-C, Error bars represent ±SEM from three biological replicates, * = p≤ 0.05 and *** = p≤ 0.001.

(E-H) Wild type immunization C57BL/6 mice (n=3) were immunized s.c. with 300 μg of OVA protein or PBS as a control and boosted with OVA 14 days later. Draining lymph nodes were collected five days following booster immunization (day 19) and analyzed immediately. An aliquot of recovered cells was cultured post-recovery and analyzed on day

five. (**E)** Mean frequency of trog^{+} CD4^{+} T cells from PBS injected *(left)* and OVA-immunized *(center)* mice immediately following recovery. *(Right)* The frequency of trog^{+} CD4^{+} T cells from OVA-immunized mice after a day five culture *in vitro*. **(F)** Representative histogram overlays showing levels of CD69 in CD4^{+} T cells *(left)* and the expression of GATA-3 *(middle)* and IL-4 *(right)* in trog^{+} *(thick black line)* and trog^{-} *(thin black line)* CD69^{High} CD4^{+} T cells. CD4^{+} T cells from PBS control mice are shown in shaded grey. **(G-H)** Frequency of (G) GATA-3 and (H) IL-4^{+}, trog^{+} *(black)* and trog^{-} *(grey)* CD69^{High} CD4^{+} T cells recovered from OVA immunized mice. For histograms, dotted vertical lines represent the maximum fluorescence intensity of 99% of CD4^{+} cells stained with respective isotype controls. In Figs. E, G and H, error bars represent ±SEM from three biological replicates, * = $p \leq 0.05$, ** = $p \leq 0.01$ and *** = $p \leq 0.001$. Data is representative of at least two separate experiments.